3-D recursive extrapolation operators

Jan Thorbecke [1]

8.1 Introduction

To visualize the 3-D subsurface of the earth 3-D migration algorithms are needed which give accurate results within a reasonable computation time. In this Chapter several recursive depth migration algorithms are discussed and compared with each other. The backbone of every recursive depth migration algorithm is a 3-D extrapolation algorithm. In lateral homogeneous media the extrapolation algorithm can be a simple multiplication in the wavenumber domain, but extrapolation through 3-Dimensional inhomogeneous media is a more computation intensive operation and requires a space-variant spatial convolution. Recently various authors (Holberg (1988), Blacquière (1989), Hale (1991b), Soubaras (1992), Sollid and Arntsen (1994), Gaiser (1994), Biondi and Palacharla (1994) and Kao et al (1994)) have published articles which pay attention to an optimized calculation and efficient implementation of 3-Dimensional extrapolation operators in a recursive depth migration. This Chapter will give an overview of the existing methods and introduces several efficient optimization and implementation methods that have not yet been discussed in the Geophysical literature (a more detailed overview is available from internet (Thorbecke, 1995)). The computation times of the different algorithms are compared with each other and the performance of the extrapolation algorithm is checked with the aid of a simple synthetic experiment.

8.2 Wave field extrapolation in the space-frequency domain

In laterally homogeneous media the recursive one-way extrapolation operator in the k_x, k_y-ω (wavenumber-frequency) domain can be well represented by the phase shift operator (Gazdag, 1978):

$$\tilde{F}(k_x, k_y, \omega, \Delta z) = \exp\left(-j\sqrt{\frac{\omega^2}{c^2} - (k_x^2 + k_y^2)}\Delta z\right) \tag{8.1}$$

[1] E-mail: J.W.Thorbecke@CTG.TUDelft.NL

with Δz being a small extrapolation step. The advantage of computation in the k_x, k_y-ω domain is that the desired result is obtained by *multiplication* of the data with the phase shift operator. However, to allow laterally varying medium functions a space variant *convolution* operator in the x, y-ω (space-frequency) domain should be used. When the spatial extrapolation operator is used in an explicit recursive depth migration algorithm it must be calculated in such a way that it gives reliable and stable results within a reasonable computation time. To arrive at this goal two steps must be taken; the first step is an optimum design of the spatial operator and the second step deals with a fast implementation of the spatial convolution. It turns out that the most efficient algorithms combine these two steps and design a spatial operator in such a way that it can be implemented in a fast way.

A **first** subdivision between the different extrapolation methods can be made with respect to the type of expansion of the analytical phase shift operator (equation (8.1)) in the wavenumber domain. This expansion can be a (Taylor) series expansion of the analytical phase shift operator with respect to $k_z = \sqrt{k^2 - (k_x^2 + k_y^2)}$ (Thorbecke, 1995), an expansion with respect to $k_r^2 = k_x^2 + k_y^2$ (Berkhout, 1982), (Soubaras, 1992), (Sollid and Arntsen, 1994), (Hoff, 1995) or an expansion with respect to the cosine terms of the 1-D Fourier transformation (Hale, 1991a). In equations (8.4) to (8.6) these different approximation to the phase shift operator are shown

$$\tilde{F}_0(k_x, k_y) = \exp\left(-jk_z\Delta z\right) \tag{8.2}$$

$$\approx \sum_{m=0}^{M}\sum_{n=0}^{N} F_{mn}\cos\left(k_x m\Delta x\right)\cos\left(k_y n\Delta y\right) \tag{8.3}$$

$$\approx \sum_{m=0}^{M} F_m\cos\left(k_r m\Delta x\right) \tag{8.4}$$

$$\approx \sum_{m=0}^{M} a_m[k_x^2 + k_y^2]^m \tag{8.5}$$

$$\approx \sum_{m=0}^{M} b_m[k_z]^m \tag{8.6}$$

Equation (8.3) is the direct method which calculates the 2-D extrapolation operator F_{mn} by a one-step optimization method and can be regarded as a weighted expansion in 2-Dimensional cosine terms. The direct method requires a full 2-Dimensional spatial convolution. Equation (8.4) is a reduction of the 2-Dimensional filter problem to a 1-Dimensional filter problem by using the circular symmetry of the 2-D operator and is represented by an expansion in 1-Dimensional cosine terms. The 1-Dimensional filter problem, to obtain F_m, can be solved with a preferred 1-D optimization method (Thorbecke and Rietveld, 1994). The 1-D cosine terms are approximated by small 2-Dimensional convolution filters.

Equation (8.5) and (8.6) are expansions of the operator in non-spectral polynomials. The terms a_m and b_m in the series expansions can be obtained by calculating the coefficients from a Taylor expansion (Berkhout, 1982), or optimizing the coefficients with an error definition in a preferred norm (for example the L_2 or L_∞ norm (Parks and Burrus, 1987), (Powell, 1981)). The basic polynomials $k_x^2 + k_y^2$ and k_z which occur in equations (8.5) and (8.6) are approximated by short and accurate convolution operators.

expansion
$\cos(k_x)\cos(k_y)$
$\cos(\sqrt{k_x^2+k_y^2})$
$\sqrt{k^2-(k_x^2+k_y^2)}$
$k_x^2+k_y^2$

optimization
Least Squares
Weighted Least Squares
Non-Linear
Remez Exchange

implementation
2-D convolution
1-D convolution
Chebyshev
Series

Table 8.1 *Three criteria which are used to discriminate between different 3-Dimensional extrapolation algorithms. Note that in principle many combinations between the elements in the three blocks are possible.*

A **second** subdivision between the different extrapolation algorithms can be made with respect to the kind of optimization method used to obtain the spatial convolution operator. The type of implementation of the spatial convolution is a **third** criterion to discriminate between the different methods. Table 8.1 gives an overview of the different techniques which can be used in the expansion, optimization and implementation. Note that in principle many combinations between the elements in the three blocks are possible. For example Holberg (1988) and Blacquière (1989) use a non-linear optimization technique for the operator optimization in a 2-Dimensional cosine series (weighted inverse Fourier transformation according to equation (8.3)) and have implemented this operator as a full 2-D convolution. Hale (1991a) makes use of the McClellan transformation in equation (8.4) and uses the coefficients of a 1-D convolution operators in a Chebyshev recursion scheme. Soubaras (1992) uses the Remez exchange algorithm in the optimization of the 1-D convolution operators and in the optimization of the expansion factors (with respect to powers of $k_x^2 + k_y^2$) of the phase shift operator in equation (8.5). In this Chapter the weighted least squares optimization method is introduced as a fast alternative method for the optimization of the 2-D convolution operators and in the optimization of the coefficients in the series expansions. The McClellan method is discussed in detail and several schemes are given which optimize the original McClellan method. The series expansions with respect to k_z and $k_x^2 + k_y^2$ given in equation (8.5) and (8.6) are worked out in detail and compared with the other extrapolation methods.

8.3 Direct method

The most straightforward method which does not make use of any series expansion is called, after Berkhout (1982), the direct method. In the direct method the optimization for the convolution operator is defined by the Fourier transformation from wavenumber to spatial domain and implemented by means of an optimization scheme (see Holberg (1988) and Blacquière (1989) for the results with a non-linear optimization scheme). The advantage of the direct method is the uncomplicated optimization of the operator and the simple implementation. A disadvantage of this direct method is that in the space-frequency domain the full 2-D convolution has to be carried out for every spatial position. For an operator with a typical operator size of 25×25 points this means 625 complex multiplications and summations for every grid point! By using

the even symmetry in the operator the number of multiplications can be reduced by a factor of 4 by folding the data into a quarter and application of the convolution to this folded part. However the number of flops remains high, especially when we take into account that this convolution has to be carried out for every grid point, for every frequency of interest and for several depth steps. In this Chapter the results obtained with the direct method are used as a reference result for comparison with the other, non-direct, methods.

8.3.1 Weighted Least Squares optimization

The most simple way to obtain space-frequency operators is an inverse Fourier transformation of the exact operators from the wavenumber-frequency domain back to the space-frequency domain. Despite of its simple form this solution is not very efficient because the spatial convolution operator obtained in this way must be very long to give stable and accurate results. Tapering the spatial operator gives some improvements (Nautiyal et al., 1993) but for accurate extrapolation results tapering cannot be used as pointed out by Thorbecke and Rietveld (1994). The aim in the design of the operator is a short convolution operator with a wavenumber-frequency spectrum which is, over a desired wavenumber band, equal or close to the exact phase shift operator in the k_x, k_y-ω domain. The starting point in the analysis of this optimization problem is the inverse Fourier transformation which is defined as

$$\tilde{F}(k_x, k_y) = \int \int_{-\infty}^{\infty} F(x, y) \exp(jk_x x) \exp(jk_y y) dx\ dy \tag{8.7}$$

Using the discrete version of the Fourier integral and the even symmetry in the phase shift operator equation (8.7) is rewritten in a discrete equation as (Blacquière, 1989)

$$\tilde{F}(k_x, k_y) \approx \sum_{m=0}^{M} \sum_{n=0}^{N} S_{mn} F(m\Delta x, n\Delta y) \cos(k_x m\Delta x) \cos(k_y n\Delta y) \tag{8.8}$$

with S_{mn} defined as

$$S_{mn} = \begin{cases} 1 & \text{for } m = n = 0, \\ 2 & \text{for } m = 0 \vee n = 0, \\ 4 & \text{for } n \neq 0 \wedge m \neq 0 \end{cases} \tag{8.9}$$

Using the Circular symmetry in the operator by interchanging n and m and the fact that $\sum_{m=0}^{M} \sum_{n=0}^{m} = \sum_{n=0}^{N} \sum_{m=n}^{M}$ the number of equations can be further reduced to 1/8 of the original number of equations (this reduction is only possible if $\Delta x = \Delta y$)

$$\begin{aligned} \tilde{F}(k_x, k_y) \approx \sum_{m=0}^{M} \sum_{n=0}^{m} F(m\Delta x, n\Delta y) \Big[& S_{mn} \cos(k_x m\Delta x) \cos(k_y n\Delta y) \\ & + S'_{nm} \cos(k_x n\Delta x) \cos(k_y m\Delta y) \Big] \end{aligned} \tag{8.10}$$

with S'_{nm} defined as

$$S'_{nm} = \begin{cases} 0 & \text{for } n = m, \\ 2 & \text{for } n = 0 \vee m = 0, \\ 4 & \text{for } m \neq 0 \wedge n \neq 0 \end{cases} \tag{8.11}$$

and $M \times N$ being the user specified size of the desired short operator. Using the shorter matrix notation equation (8.10) can be rewritten as

$$\tilde{\mathbf{F}}' = \underset{\sim}{\Gamma}\mathbf{F} \tag{8.12}$$

with $\mathbf{F}$ the desired short operator and $\tilde{\mathbf{F}}'$ being its spatial Fourier transform, yielding an approximation of the exact phase shift operator. Equation (8.8) with the quarter, or equation (8.10) with the octal part has to be solved for the unknown operator coefficients $F_{mn} = F(m\Delta x, n\Delta y))$ for all wavenumbers (k_x, k_y) of interest. Therefore a weighted error function $\tilde{\varepsilon}$ is defined as

$$\tilde{\varepsilon} = \tilde{\mathbf{E}}^{\mathbf{h}} \underset{\sim}{\tilde{\Lambda}} \tilde{\mathbf{E}} \tag{8.13}$$

with

$$\tilde{\mathbf{E}} = \underset{\sim}{\Gamma}\,\mathbf{F} - \tilde{\mathbf{F}} \tag{8.14}$$

and $\underset{\sim}{\tilde{\Lambda}}$ a diagonal matrix containing a weighting function on its diagonal. The introduced weighting function gives a good control over the desired functionality of the space-frequency operators. The least-squares solution of equation (8.13) is given by

$$\mathbf{F} = \left[\underset{\sim}{\Gamma}^h \, \underset{\sim}{\tilde{\Lambda}} \, \underset{\sim}{\Gamma}\right]^{-1} \underset{\sim}{\Gamma}^h \, \underset{\sim}{\tilde{\Lambda}} \, \tilde{\mathbf{F}} \tag{8.15}$$

where $\underset{\sim}{\Gamma}^h \, \underset{\sim}{\tilde{\Lambda}} \, \underset{\sim}{\Gamma}$ is a square matrix. The weighted least-squares method (abbreviated as WLSQ) can be used in the calculation of short (2-D) spatial convolution operators but also in the calculation of series expansion factors. In DELPHI Volume V (1994), Appendix A, the WLSQ method was used to solve the 1-D optimization problem. For the 1-D optimization problem the WLSQ method has another advantage; the matrix $\underset{\sim}{\Gamma}^h \, \underset{\sim}{\tilde{\Lambda}} \, \underset{\sim}{\Gamma}$ which has to be inverted has a Toeplitz structure and can be inverted fast by using the Levinson scheme. For the 2-Dimensional problem standard LINPACK routines are used to calculate a QR decomposition of the matrix $\underset{\sim}{\Gamma}^h \, \underset{\sim}{\tilde{\Lambda}} \, \underset{\sim}{\Gamma}$ and with this decomposition the solution of matrix equation (8.15).

8.3.2 Impulse response of an extrapolation operator

An impulse response experiment is used to test the behavior of the extrapolation operator in an explicit finite-difference migration algorithm. In the middle of a spatial limited homogeneous

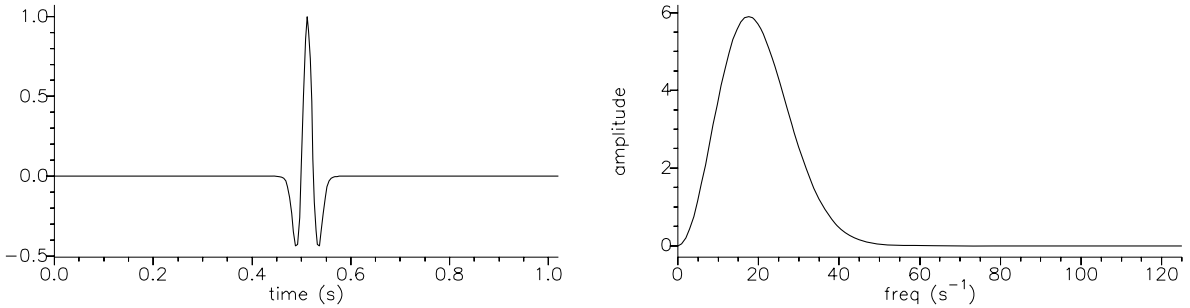

a) Time signature b) Amplitude spectrum

Fig. 8.1 *a) Time signature and b) Amplitude spectrum of the wavelet used in the migration experiments.*

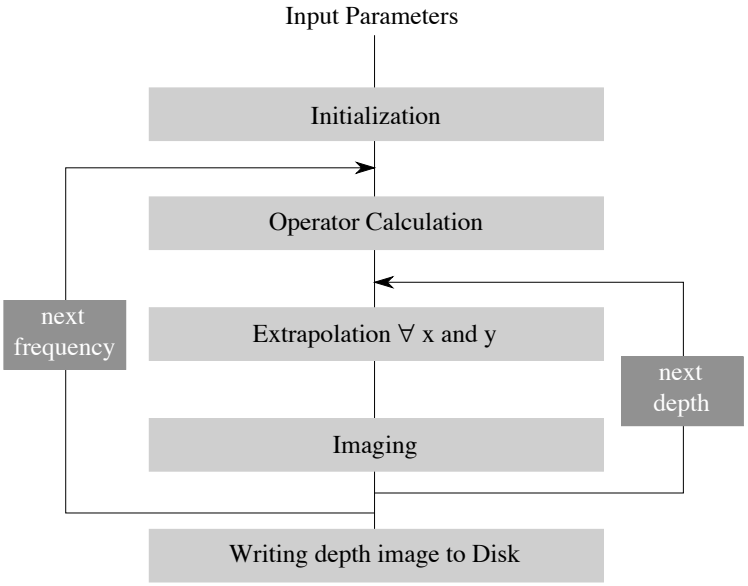

Fig. 8.2 *Processing scheme for the impulse response experiment. Note that the extrapolation block in the scheme is different for every different extrapolation implementation.*

medium a point source is defined with the source signature shown in Figure 8.1. The zero-phase Ricker wavelet is centered at 0.512 seconds. The constructed data set is transformed to the frequency domain and extrapolated to deeper depth levels for every frequency of interest. At every depth level an imaging step is carried out and the depth image is stored in memory. At the end of the calculation for all frequencies the final depth image is written to disk. The block-scheme of this algorithm is shown in Figure 8.2. For the other extrapolation algorithms discussed in this Chapter the extrapolation block in Figure 8.2 is replaced with the extrapolation algorithm of interest, everything else in the scheme remains the same. For the synthetic experiment the following parameters are used: $c = 1000ms^{-1}$, $f_{min} = 5Hz$ and $f_{max} = 45Hz$, $\Delta x = \Delta y = \Delta z = 10m$, $\Delta t = 0.004s$ and 55 depth steps are taken on a x,y grid of 111×111 samples wide. Note that the maximum frequency is positioned in the wavenumber domain at $0.9 * \frac{\pi}{\Delta x} (= k_N)$.

A reference output of this experiment can be calculated by using the exact expression of the extrapolation operator in the spatial domain. The exact spatial operator is defined by the dipole pulse response which is given by

$$G_0(x, y, z, \omega) = \frac{1 + jkr}{r^2} \cos\phi \exp(-jkr) \tag{8.16}$$

with $k = \frac{\omega}{c}$, $\cos\phi = \frac{z}{r}$ and $r = \sqrt{z^2 + x^2 + y^2}$. Using the complex conjugate G_0^* of the dipole response in a non recursive version of the scheme given in Figure 8.2 a reference impulse response can be calculated for the synthetic model described above.

Every horizontal slice in the constructed depth image corresponds to a certain dip angle. For example for a depth slice at 200 m the dip angle is given by $\cos\phi = z(ct_0)^{-1} \Rightarrow \phi \approx 67^o$. In Figure 8.3 three cross sections out of the 3-D depth image of the reference experiment are shown;

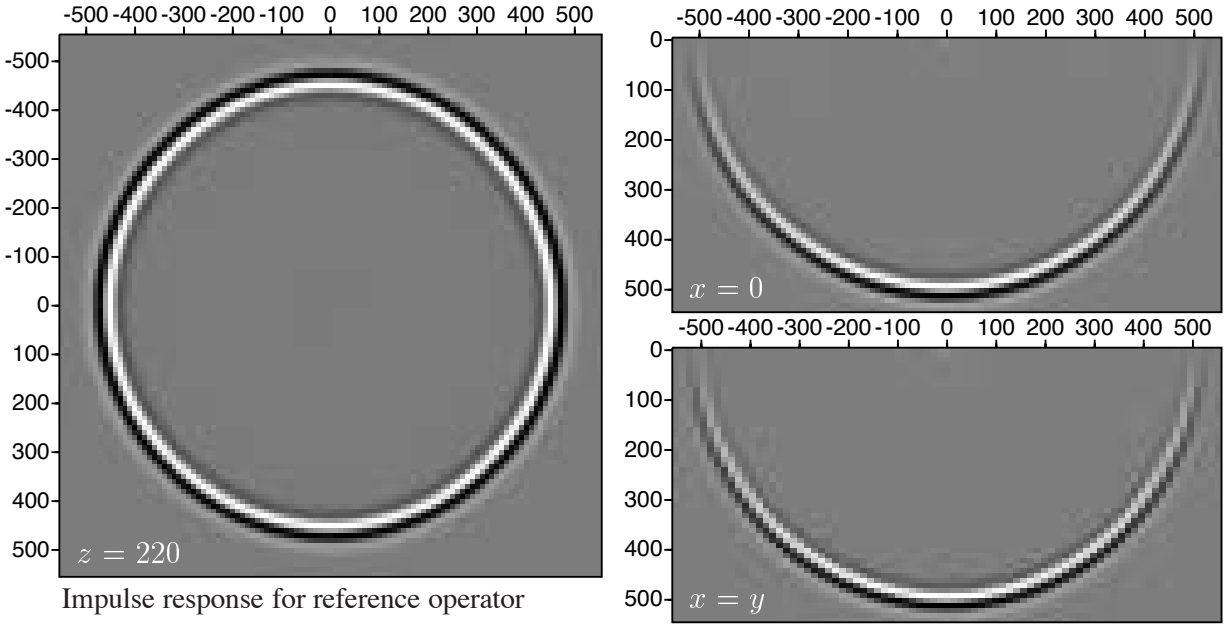

Fig. 8.3 *Reference output for the migration experiment with left the depth slice at z = 220 m. Top right shows a vertical slice for x=0 and bottom right a vertical slice for x=y. Note the perfect circular shape and the accuracy at the higher angles.*

the right pictures in Figure 8.3 show a vertical cross section for x=0 (top) and x=y (bottom), the left hand side picture in Figure 8.3 shows a horizontal cross section at a depth of 220 m which corresponds to a reflector dip of 65 degrees.

Using 2 Dimensional 19×19 convolution operators obtained with the introduced WLSQ method gives the depth image shown in Figure 8.4a. In the spatial convolution scheme the even symmetry in the operator is used explicitly by folding the data into common operator point parts, which reduces the number of multiplications significantly. In the calculation of the convolution operator only 1/8 th of the total spectrum is used by making use of the circular symmetry and the fact that $\Delta x = \Delta y$. In Figure 8.4a we see that the artefacts in the depth image consists of inner 'circular' events at the higher angles which have a square structure. This square structure is due to the fact that the solution of the optimization problem is calculated on a rectangular grid. In the presentation of the paper of Kao et al (1994) similar features were observed. Using a longer 2-D convolution operator of 31×31 points as shown in Figure 8.4b these rectangular artefacts have vanished. A more detailed discussion of the errors in the extrapolation operators is given in the next subsection. In section 8.6 the computation times for the direct convolution method is given for different operator sizes on different machines used in our research group.

8.3.3 Error analysis

From an engineering point of view it is interesting to investigate how the different parameters in the optimization procedure must be chosen to obtain efficient operators which are accurate up to a desired maximum angle. For this analysis it is necessary to define accuracy in a useful way. In Powell (1981) the most common used definitions of accuracy are given. In this section

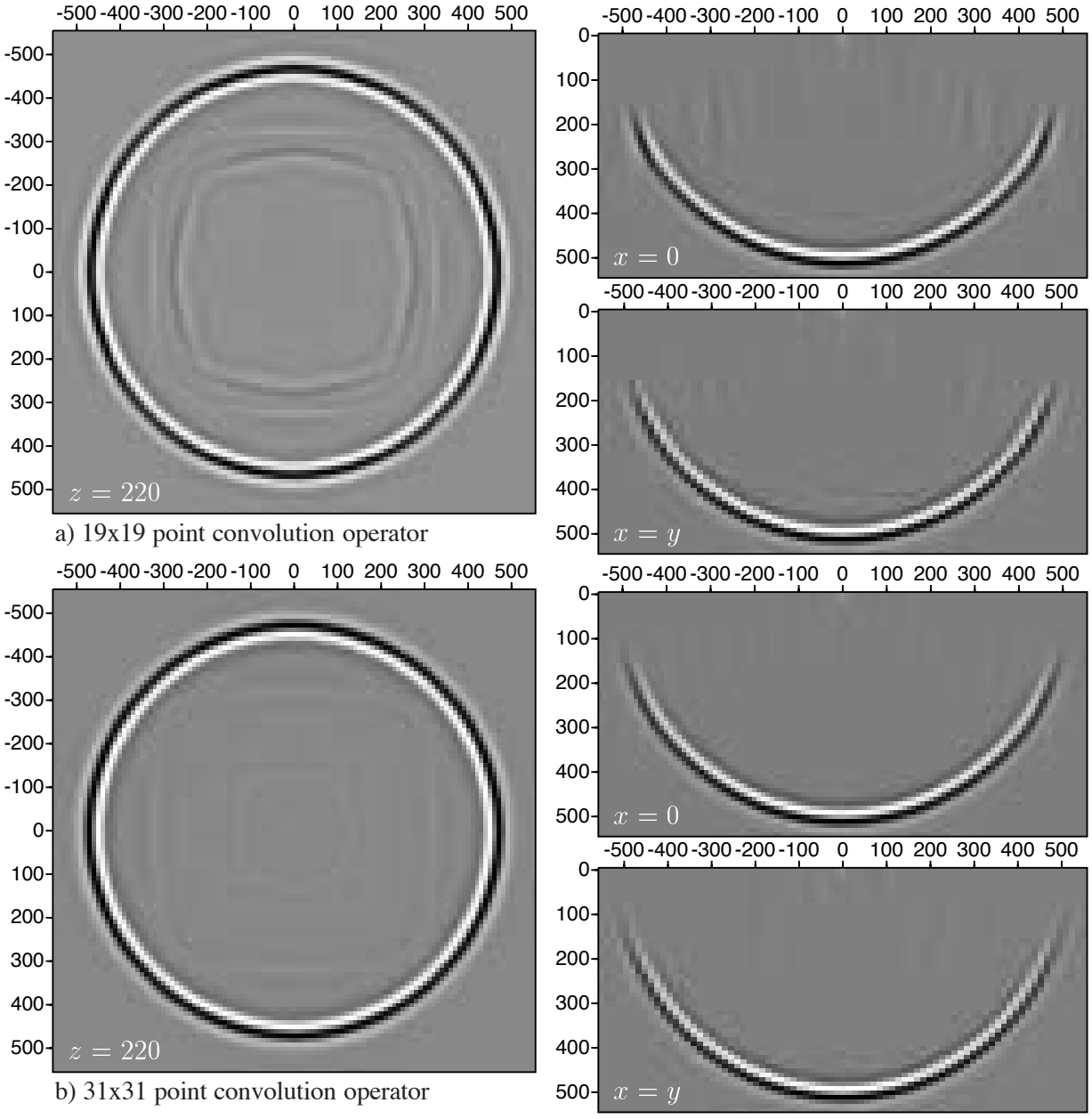

a) 19x19 point convolution operator

b) 31x31 point convolution operator

Fig. 8.4 *Results of the WLSQ optimized operators for different operator sizes. Note that the artefacts which are present in the result for the 19x19 operator disappear for the larger operator size.*

we will use the L_2 and the L_∞ norms to calculate accuracy in a certain domain of interest. The domain of interest is defined by $k_r < k \sin(\alpha_{max})$ $(= k_{r,max})$ with $k = \frac{\omega}{c}$.
Based on the results of many experiments the following L_2 and L_∞ error norms are defined over the domain of interest

$$\varepsilon_2 = \left[\frac{\int_{\phi=0}^{\frac{\pi}{4}} \int_{k_r=0}^{k_{r,max}} \| F(k_r) - \hat{F}(k_r,\phi) \|^2 k_r \, dk_r \, d\phi}{\int_{\phi=0}^{\frac{\pi}{4}} \int_{k_r=0}^{k_{r,max}} \| F(k_r) \|^2 k_r \, dk_r \, d\phi} \right]^{\frac{1}{2}} \tag{8.17}$$

$$\varepsilon_\infty^a = \max_{0 \le k_r \le k_{r,max}} | \, \| F(k_r) \| - \| \hat{F}(k_r) \| \, |$$

$$+ \max_{k_{r,max} < k_r \leq k_N} \mid 1 - \|\hat{F}(k_r)\| \mid \quad \{\text{if } \|\hat{F}(k_r)\| > 1.0\} \tag{8.18}$$

$$\varepsilon^p = \left[\int_{\phi=0}^{\frac{\pi}{4}} \int_{k_r=0}^{k_{r,max}} \| \frac{\partial E_p}{\partial k_r} \; k_r \|^2 \; dk_r \; d\phi \right]^{\frac{1}{2}} \tag{8.19}$$

with

$$E_p = \arg F(k_r) - \arg \hat{F}(k_r, \phi)$$

where $\hat{F}(k_r)$ is an approximation to the true function $F(k_r)$, ε_2 is the normalized least squares error, ε^a_∞ the maximum amplitude error and ε^p a measurement for the derivative of the phase error with respect to the polar distance k_r . The normalized ε_2 error is a global error and is related to the accuracy of the operator. The amplitude error gives an indication of the stability of the operators in a recursive extrapolation scheme. Note that $\|F(k_r)\|^2 = 1$ in the domain of interest. Included in the ε^a_∞ error is a stability measurement for $k \sin(\alpha_{max}) < k_r \leq k_N$. If the amplitude of the operator in this domain is higher than 1.0 then it contributes to the ε^a_∞ error. The ε^p error is defined in such a way that it is sensitive to errors in the circular symmetry of the operator. In the ideal case the ε^p error should be zero because of the circular symmetry of the operator. To compute the derivative with respect to k_r a three point finite difference operator is used to compute the derivative with respect to k_x and k_y. With these derivatives the $\frac{\partial}{\partial k_r} = \frac{\partial}{\partial k_x}\frac{\partial k_x}{\partial k_r} + \frac{\partial}{\partial k_y}\frac{\partial k_y}{\partial k_r}$ is calculated.
To determine the errors due to the recursive use of the operator in a homogeneous medium (which is a worst case situation) the difference with respect to the reference impulse response is calculated for every depth slice according to

$$\varepsilon_s(z) = \left[\frac{\int_{x=0}^{x_{max}} \int_{y=0}^{y_{max}} \left\| F(x,y,z) - \hat{F}(x,y,z) \right\|^2 \; dx \; dy}{\int_{x=0}^{x_{max}} \int_{y=0}^{y_{max}} \|F(x,y,z)\|^2 \; dx \; dy} \right]^{\frac{1}{2}} \tag{8.20}$$

This spatial error can be presented in an error curve as function of the angle (=depth). The calculation of the wavenumber errors in equation (8.17), (8.18) and (8.19) gives three values for one operator defined for one frequency. For a more useful definition three frequencies, within the

Operator			**20 Hz**			**Average**		
angle	size	weight	ε_2	ε^a_∞	ε^p	$\bar{\varepsilon}_2$	$\bar{\varepsilon}^a_\infty$	$\bar{\varepsilon}^p$
15	5x5	1e-5	1.6e-3	3.2e-3	1.6e-5	2.4e-3	2.2e-3	7.1e-5
30	9x9	2e-5	1.4e-3	3.0e-3	5.6e-4	1.9e-3	2.9e-3	2.7e-4
45	13x13	4e-5	1.0e-3	3.3e-3	3.5e-4	1.5e-3	3.1e-3	3.9e-4
60	19x19	4e-5	1.2e-3	2.4e-3	1.6e-3	1.5e-3	2.9e-3	1.2e-3
75	31x31	6e-5	1.7e-3	1.2e-3	4.8e-3	1.9e-3	1.4e-3	4.3e-3

Table 8.2 *Optimum operators which are accurate up to a maximum angle of interest. Note that for small angles these operators are stable but don't suppress all higher angles*

frequency range of interest, are analyzed: one at a low frequency (in our example 5 Hz.), a central frequency (20 Hz) and at a high frequency (40 Hz.). The error in the operator can be varied by changing the weighting function, the operator length and the maximum angle of interest.

From these experiments described above and given in detail in Thorbecke (1995) we have developed a criterion which can be used to determine if a certain operator calculation method gives stable and accurate results in a recursive extrapolation algorithm. To use this criterion the wavenumber spectrum of the operator must be calculated for three characterizing frequencies and the ε_2, ε^a_∞ and ε^p errors have to be calculated for every frequency. These errors must then obey the following relations;

- $\bar{\varepsilon}_2 \leq 2e^{-3}$ accuracy measurement
- $\varepsilon^a_\infty \leq 3e^{-3}$ stability measurement
- $\varepsilon^p \leq 1e^{-2}$ circularity measurement

Given the error criteria we can now determine how the weight factor and the operator size must be chosen for a maximum angle of interest. The results of these experiments are summarized in Table 8.2. The small angles 15^o and 30^o are difficult to optimize for the given maximum angle, but by choosing a slightly bigger angle the operator can become stable and accurate for the smallest operator size possible. For example to get the operator for 30^o a maximum design angle of 40^o degrees has to be chosen. If one wants to design operators with small maximum angles of interest and suppression of all the higher angles a larger operator size must be chosen than the one given in Table 8.2. The larger $\bar{\varepsilon}^p$ error in the 75^o operators is not as bad as it looks, the largest error peaks are positioned at the edges of the domain of interest.

Note that for small operator sizes the higher frequencies are more sensitive to errors and for the larger operators the lower frequencies are more sensitive to errors. This behavior is related to the WLSQ optimization method. A very small operator has a limited number of 'error' peaks in the frequency domain due to the limited number of contributing wavenumber components. The WLSQ optimization method with a limited number of wavenumber components cannot have very large peaks (Berkhout, 1984). If there are more wavenumber components the WLSQ method can build up large peaks in the error function (Gibbs phenomenon).

8.4 McClellan transformation

The McClellan transformation transforms a 1-D convolution operator to a 2-D convolution operator with a certain symmetry. This transformation is of interest because the implementation is simple and the computation of the transformation coefficients can be done efficiently. Hale (1991a) introduced the McClellan transformation into the Geophysical world and described two related techniques which can replace the direct 2-Dimensional spatial convolution: (1) transformation of the *non-recursive* 1-Dimensional symmetrical filter in a 1-Dimensional *recursive* filter by using the Chebyshev recursion formula (see Parks (1987), Johnson and Riess (1977), Ralston (1967), Kogbetliantz (1960), Powell (1981)), (2) the McClellan transformation of a 1-Dimensional filter to a circular symmetric 2-Dimensional filter. We will first discuss the transformation from a 1-Dimensional filter to a 2-Dimensional filter. Next the Chebyshev recursion

formula is explained and at the end of this section several methods are discussed which optimize the steps and coefficients used in the McClellan transformation.

McClellan Transformation from 1-D to 2-D

If the operator has a circular symmetry it is possible to reduce the computation time of the 2-Dimensional filter by means of a McClellan transform. The McClellan transform (McClellan, 1973) defines a mapping from a 1-D wavenumber axis to the 2-D wavenumber domain. The change of variables to be described depends on the fact that both the operator approximations in 1 and 2-Dimensions can be written as sums of cosine functions. The 1-Dimensional filter problem of an even symmetrical operator can be rewritten as (note the similarity with equation (8.8))

$$\tilde{F}(k_r) \approx F(0) + 2 \sum_{m=1}^{M} F(m\Delta x) \cos{(k_r m \Delta x)} \tag{8.21}$$

$$\tilde{F}(k_r) \approx \sum_{m=0}^{M} F'(m\Delta x) \cos{(k_r m \Delta x)} \tag{8.22}$$

$$\tilde{F}(k_r) \approx \sum_{m=0}^{M} \hat{F}(m\Delta x) \cos{(k_r \Delta x)}^m \tag{8.23}$$

with the choice of a suitable set of coefficients $\hat{F}(m\Delta x)$ that approximate the 1-D extrapolation operator $\tilde{F}(k_r)$. In equation (8.22) $F'_m = 2F_m$ for $m = 1, \ldots M$ and $F'_m = F_m$ for $m = 0$. The last step from equation (8.22) to equation (8.23) can be seen by letting $\phi = \cos{(k_r \Delta x)}$. Then $\cos{(k_r m \Delta x)} = \cos{(m \arccos{(\phi)})} = T_m(\phi)$, where $T_m(\phi)$ is the Chebyshev polynomial of order m. Each cosine term in equation (8.22) may then be expressed in the form

$$\cos{(k_r\ m\Delta x)} = \sum_{n=0}^{N} \alpha_{m,n} \cos{(k_r \Delta x)}^m \tag{8.24}$$

where the $\alpha_{m,n}$ are real coefficients and easily obtained with the Chebyshev recursion formula. Equation (8.22) reduces then further to

$$\tilde{F}(k_r) \approx \sum_{m=0}^{M} F'(m\Delta x) T_m(\phi) = \sum_{m=0}^{M} \hat{F}(m\Delta x) \phi^m \tag{8.25}$$

where both right-sides of the equation are now polynomials in ϕ.

The cosine terms in equation (8.23) can be approximated by a 2-Dimensional filter (assuming $\Delta x = \Delta y$)

$$\cos{(k_r\ \Delta x)} \approx \sum_{p=0}^{P} \sum_{q=0}^{Q} c_{pq} \cos{(k_x\ p\Delta x)} \cos{(k_y\ q\Delta y)} \tag{8.26}$$

where c_{pq} are called the McClellan factors (McClellan, 1973). By making the substitution of equation (8.26) into equation (8.23) it reduces to

$$\tilde{F}(k_r) \approx \sum_{m=0}^{M} \sum_{n=0}^{N} \ddot{F}(m\Delta x, n\Delta y) \cos{(k_x \Delta x)}^m \cos{(k_y \Delta y)}^n \tag{8.27}$$

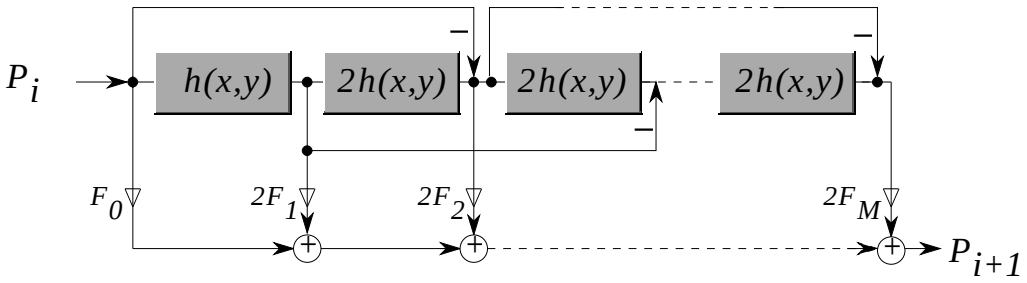

Fig. 8.5 *Chebyshev recursion scheme. The $h(x, y)$ boxes represent the 2-D McClellan transformation of $\cos(k_r)$, F_m represents the coefficients of the 1-D convolution operator.*

which can be put in the form (using Chebyshev's recursion formula again)

$$\tilde{F}(k_r) \approx \sum_{m=0}^{M} \sum_{n=0}^{N} \breve{F}(m\Delta x, n\Delta y) \cos(k_x\ m\Delta x) \cos(k_y\ n\Delta y) \tag{8.28}$$

which is the desired form for a 2-Dimensional filter which was already shown in equation (8.8) (Note that $\ddot{F}$ and $\breve{F}$ are scaled versions of F). For example for $P = Q = 1$ the transformation for circular symmetry reduces to a 9-term McClellan convolution operator (also called a first order approximation) which is given by Hale (1991a) where $-c_{00} = c_{10} = c_{01} = c_{11} = 0.5$ and

$$\cos(k_r\ \Delta x) \approx -1 + 0.5(1 + \cos(k_x \Delta x))(1 + \cos(k_y \Delta y)). \tag{8.29}$$

$P = Q = 2$ gives a 25-term McClellan transform (second order approximation) which is also given by Hale (1991a). The McClellan factors c_{pq} can be derived by defining points in the k_x, k_y plane which map to a point on the k-axes of the 1-D operator such that all coefficients are uniquely defined (for the first order McClellan approximation 4 points are needed). The problem with the McClellan transform, given the original McClellan factors in equations (8.29), is that for wavenumbers closer to the Nyquist wavenumber the transformation deviates from the ideal circular shape.

Chebyshev recursion formula

The second improvement in the computation scheme is the transformation of the non-recursive 1-Dimensional filter to a 1-Dimensional recursive filter derived from the recursive formula of the Chebyshev polynomials

$$\cos(m\phi) = 2\cos(\phi)\cos((m-1)\phi) - \cos((m-2)\phi) \tag{8.30}$$

This Chebyshev filter structure is not useful for 1-Dimensional filters. Direct convolution is both simpler and more efficient. The Chebyshev structure is more advantageous for 2-Dimensional operators with an even symmetry, such as the circular symmetric extrapolation operators. The Chebyshev recursion scheme can be implemented in the computer without much effort. McClellan and Chan (1977) have analyzed this so called Chebyshev structure in detail and observed

that the scheme requires the minimum number of multiplications in comparison with the direct scheme and it is the most stable scheme with respect to the round off-noise. In Figure 8.5 a flow diagram for the Chebyshev recursion scheme is given. Note that only the coefficients of the 1-D operator are involved. Hence the number of computations depends linearly on the length N of the 1-D operator and not on N^2 as in the implementation of a direct 2-D convolution. The computation times for several 1-D operator lengths and different operators $h(x, y)$ are given in section 8.6.

In Figure 8.6 the migration results of the McClellan transformation combined with the Chebyshev recursion scheme is shown for the second order (17-term) McClellan transformation. The optimized 1-D convolution operator has a full length of 25 points and is obtained with the Remez exchange algorithm (see Powell (1981) and Thorbecke (1995) for a detailed discussion on the Remez algorithm). The Chebyshev recursion scheme makes use of the even symmetry in the operator so only 13 points of the 1-D operator are needed as expansion terms in the recursive scheme. The notation of the operator size used in Figure 8.6 gives first the number of terms in the expansion and second the size of one single term. For example the notation 13×17 means that the expansion is done in 13 terms where every term consists of an operator with 17 points.

The cross-sections in Figure 8.6 give a good view of how the McClellan transformation handles the higher angles. The noise around the source position in the x-slice is an artefact of the used 1-D operator. The 1-D Remez optimized operator is chosen because it gives, in some way, the best 1-D operator and the even symmetry of the 1-D operator is used explicitly in the optimization scheme.
Despite the deviation at the higher angles the McClellan transformation combined with the Cheby-

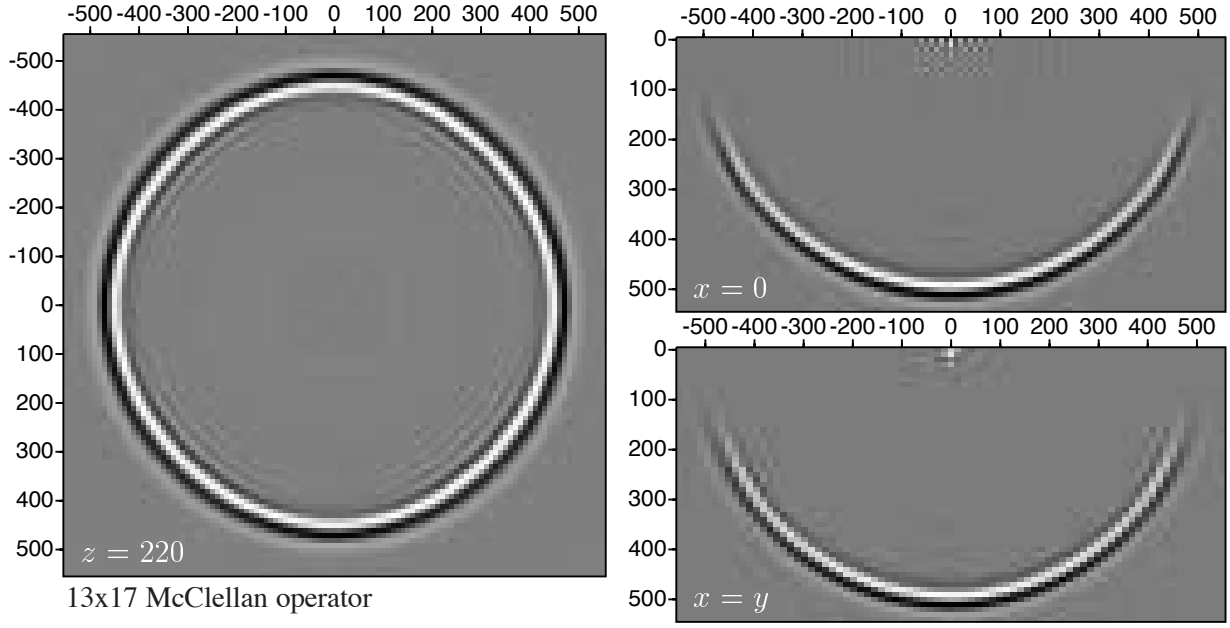

Fig. 8.6 *Depth images obtained with the original McClellan transformation. For the higher angles the McClellan operators deviate from the ideal circular shape. Note the deviation at the higher angles in the diagonal slice.*

shev recursion scheme is a very powerful and useful approach. The performance at higher angles can be improved in several ways. In the subsections 8.4.1, 8.4.2 and 8.4.3 three improvements are discussed.

8.4.1 Hazra and Reddy Coefficients

Optimizing the design of the McClellan factors c_{pq} in equation (8.26) is a good way to improve the performance of the McClellan transformation. The first order filter is of special interest because it is a small and therefore fast operator. The aim of the technique proposed by Hazra and Reddy (1986) is to make the maximum contour of interest of the 2-D operator approximate a circle with a high degree of accuracy. This better approximation is achieved by mapping an additional point of the cut-off boundary of the 2-D operator onto the cut-off boundary of the 1-D filter (the cut-off boundary is defined by the maximum wavenumber of interest). This mapping of the additional point is obtained by making the cut-off wavenumber of the 1-D filter as one of the design parameters. A consequence of this is that the wavenumber of the cut-off boundary of the 2-D operator on the k_x-axis and k_y-axis may be different from the cut-off wavenumber of the 1-D filter.

The first order original McClellan transformation maps the origin $(0, 0)$ in the (k_x, k_y) plane onto the point $k_x = 0$ of the k_x-axis in the wavenumber response of the 1-D operator. The points $(k_{x,N}, 0), (0, k_{y,N})$ and $(k_{x,N}, k_{y,N})$ from the (k_x, k_y) plane all map onto $k_x = k_{x,N}$. With the definition of these four points the coefficients in the first order McClellan transform are uniquely determined. This mapping has the following properties: (1) the contours of the McClellan transformation are approximately circular for low values of k_r and deviates considerably from circular contours as k_r increases and is square at $k_r = 1$, (2) the original McClellan transformation makes the frequency response of the 2-D operator along the k_x-axis and along the k_y-axis identical to the frequency response of the original 1-D operator. Contour lines in the original

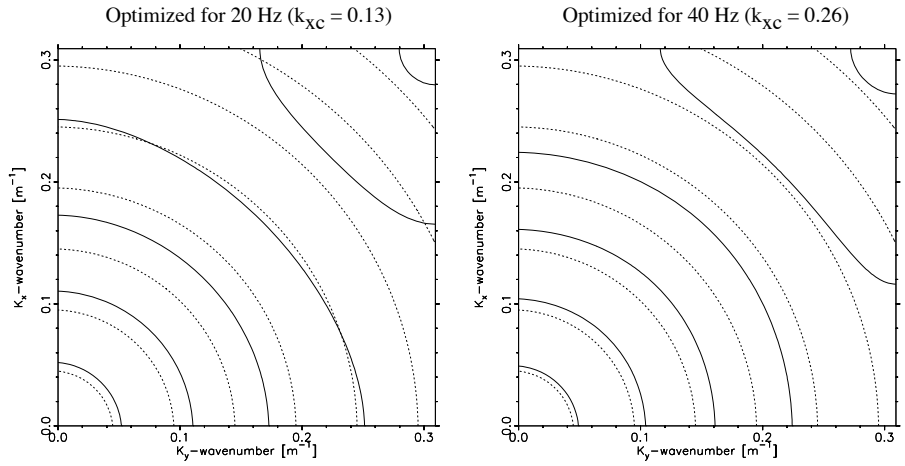

Fig. 8.7 *Contour plots of the optimized Hazra and Reddy transformation for two different frequencies. Note the circular shape and the scaling.*

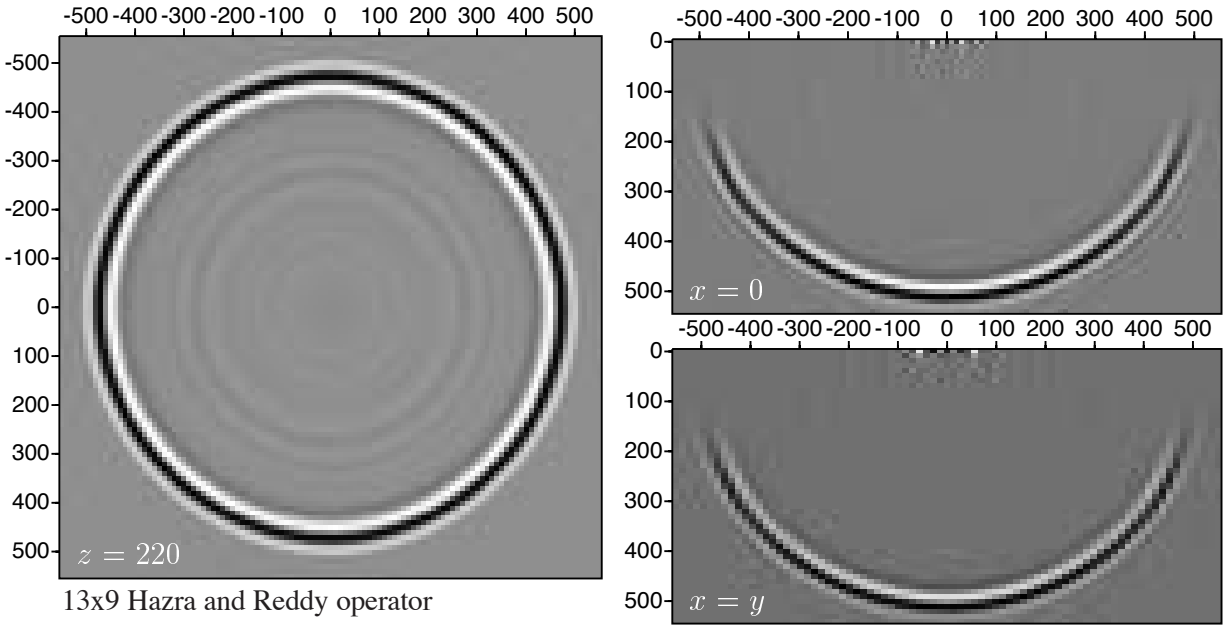

Fig. 8.8 *Depth images obtained with the optimized Hazra and Reddy transformation. Note the improvement in the circular shape in the depth slice in comparison with the original McClellan transformation.*

McClellan transformation show that the deviation from the circular contour is maximum near the neighborhood of the diagonal joining the points $(0, 0)$ and $(k_{x,N}, k_{y,N})$ in the (k_x, k_y) plane. It is possible, for a given maximum k_r, to improve the contour by forcing an appropriate point on this diagonal to be on the circular contour. With this mapping of an extra point on the circular contour, it is not possible, to make the frequency response of the 1-D operator identical to the frequency response of the original 1-D operator along the k_x-axis and along the k_y-axis. Thus the mapping of the extra point on the diagonal is only possible when the cut-off wavenumber along the k_x axes is one of the design parameters. The McClellan factors according to Hazra and Reddy are dependent on the maximum wavenumber of interest and are given by

$$c_{11} = \frac{ab - 2ac}{2bc^2},\ c_{01} = c_{10} = \frac{1}{g} - c_{11},\ c_{00} = 1 - c_{01} - c_{10} - c_{11}$$

where

$$b = \sin^2\left(\frac{k_{xc}}{2}\right),\ c = \sin^2\left(\frac{k_{xc}}{2\sqrt{2}}\right),\ g = 2 + \frac{b - 2c}{c^2},\ a = \frac{b}{g} \tag{8.31}$$

$$k_c = 2\sin^{-1}\left(\sqrt{a}\right)$$

and where k_{xc} is the maximum wavenumber of interest of the circular symmetric 2-D filter on the k_x-axis and k_c is the maximum wavenumber of interest of the 1-D operator. For a more detailed discussion on the derivation of the parameters in equation (8.32) the reader is referred to Hazra and Reddy (1986). In Figure 8.7 two contour plots are shown for two different frequencies. Up to the desired maximum value these contours are circular, outside the desired value the contours are not circular shaped. Note the scaling along the wavenumber axes.

In the extrapolation algorithm first the McClellan factors are calculated according to 8.32 for a

given k_{xc} which gives besides the optimized McClellan factors also a k_c for the 1-D operator. With this calculated k_c value the 1-D operator is designed. Note that k_c is always smaller than k_{xc}. Due to the choice of the coefficients this 1-D operator is stretched to a correct 2-D operator. To compensate for this stretch the 1-D convolution operator must be calculated with a scaled Δz. This can be explained by regarding the effect of the optimized Hazra and Reddy factors as a scaling of the k_x-axes. The 1-D phase shift operator is then given by

$$\begin{aligned} \tilde{F}(k_x) &= \exp\left(-j\ [k^2 - (\alpha k_x)^2]^{\frac{1}{2}}\ \Delta z\right) \\ &= \exp\left(-j\ [(\frac{k}{\alpha})^2 - k_x^2]^{\frac{1}{2}}\ \alpha\Delta z\right) \end{aligned} \tag{8.32}$$

where $\frac{k}{\alpha} = k_c$ and $\alpha\Delta z$ is the scaled depth step.

The migration results for the Hazra and Reddy optimized coefficients are shown in Figure 8.8. The circular shape of the depth slice is good and the artefacts at the diagonals, which were present in the original McClellan transformation, are absent. Note that the computation time of the optimized coefficients is very small, only a few multiplications and additions per frequency, so the same computation effort is required as for the original McClellan transformation which makes the method very attractive. It will be interesting to investigate if it is possible to adjust the 17-points McClellan transformation with the same method.

8.4.2 Optimized McClellan factors

The aim in optimizing the McClellan transformation is to choose the McClellan factors c_{pq} in equation (8.26) such that the contours produced by the transformation have some desired shape. For some examples it is sufficient to control the shape of one single contour. In other problems it is necessary to design the shape of the contours in a specific part of the wavenumber domain (Mersereau et al., 1976). The error function which has to be optimized for a circular contour design is given by

$$\begin{aligned} E &= M(c_{pq}, k_x, k_y) - \cos\sqrt{k_x^2 + k_y^2} \quad \text{with} \\ M(c_{pq}, k_x, k_y) &= \sum_{p=0}^{P}\sum_{q=0}^{Q} c_{pq}\cos(k_x)\cos(k_y) \end{aligned} \tag{8.33}$$

Equation (8.33) is a non-linear function of the unknown parameters, so a computation intensive non-linear optimization scheme must be used for the minimization. In the example shown in this section a non-linear optimization scheme (CFSQP, written by C.T. Lawrence, J.L. Zhou and A.L. Tits, Version 2.0, february 1994) is used. With this scheme we try to optimize several contours within the band of interest and put the constraint

$$\begin{aligned} &|\sum_{p=0}^{P}\sum_{q=0}^{Q} c_{pq}\cos(k_x\ p\Delta x)\cos(k_y\ q\Delta y)| \le 1 \\ &0 \le k_x \le k_{x,N}\ (=\ \frac{\pi}{\Delta x}), 0 \le k_y \le k_{y,N}\ (=\ \frac{\pi}{\Delta y}) \end{aligned} \tag{8.34}$$

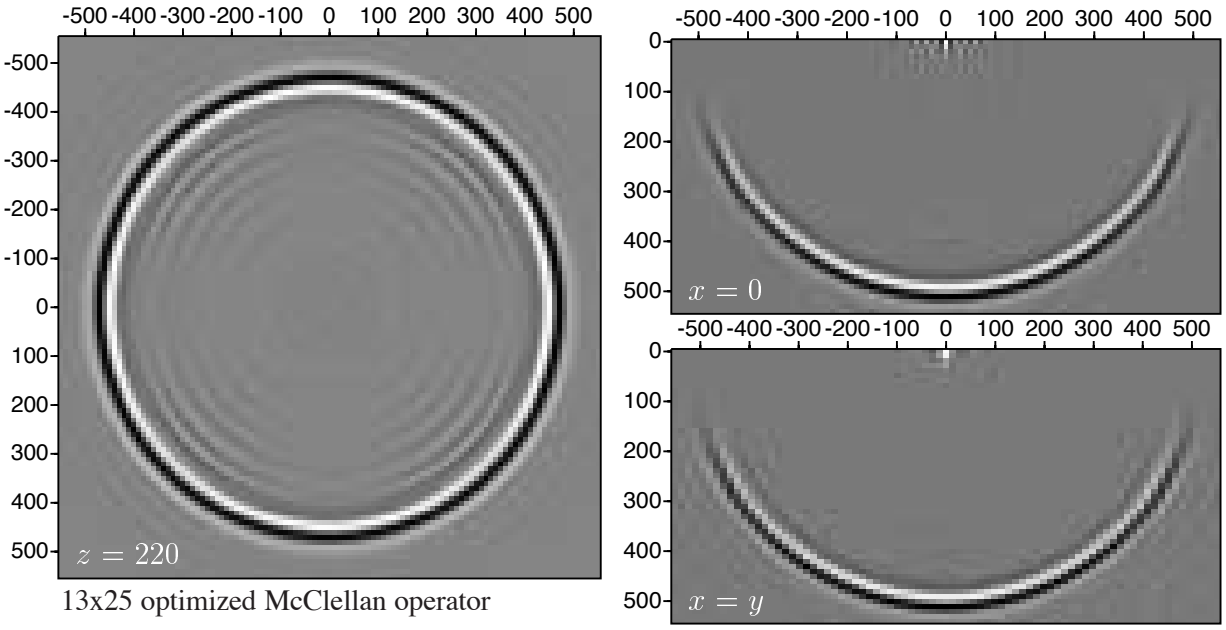

Fig. 8.9 *Depth slice at z = 220 m, a vertical slice for x=0 (top right) and bottom right a vertical slice for x=y with optimized McClellan coefficients. Note the circular shape and the small artefacts.*

for all points of the mapping in the (k_x, k_y) plane. The contours to be optimized in the objective function of equation (8.33) are defined by the maximum wavenumber value of interest. With this definition of the optimization problem the first order McClellan transformation cannot be optimized any further, but the second order transformation (25 points approximation, which means that all cross terms within the second order are used) can be improved. In the implementation of the McClellan operators we make explicitly use of the circular symmetry in McClellan operator if $\Delta x = \Delta y$. In Figure 8.9 the migration impulse response is shown for the optimized 25-point McClellan operator with frequency dependent coefficients and a 1-D operator of 25 points (13 terms). The non-linear computation time can be reduced by calculating the optimized coefficients for a wavenumber range instead of every wavenumber. In the shown example we have used only four sub domains in the total wavenumber domain of interest which keeps the time to compute the McClellan factors small. It also possible to optimize the coefficients independent of the wavenumber frequency or for different shaped McClellan filters (Blacquière, 1991).

8.4.3 Series expansion in $\cos(k_r \Delta x)$

All improvements descriped thus far make use of the Chebyshev recursion sheme, but it is also possible to use a direct expansion in $\cos(k_r \Delta x)$. To see the difference between the two schemes the Chebyshev recursion scheme and the direct scheme are written as

$$\tilde{F}(k_r) \approx \sum_{m=0}^{M} F_m T_m(\cos(k_r \Delta x)) \tag{8.35}$$

$$\approx \sum_{m=0}^{M} a_m \cos(k_r \Delta x)^m \tag{8.36}$$

$$\approx \sum_{m=0}^{M} \hat{a}_m \tilde{h}^m(k_x, k_y) \tag{8.37}$$

with

$$\tilde{h}(k_x, k_y) \approx \cos(k_r \Delta x) \tag{8.38}$$

In equation (8.37) $\tilde{h}$ (defined in equation (8.38)) is optimized first and with this approximation to $\cos(k_r \Delta x)$, $\hat{a}_m$ is optimized. In equation (8.35), the Chebychev recursion scheme, the optimization of $\cos(k_r \Delta x)$ is independent of the optimization of F_m. In the scheme of equation (8.37) a better operator can be designed, because the optimization of the series coefficients is dependent on the approximation to $\cos(k_r \Delta x)$ To optimize the $\hat{a}_m$ the WLSQ method is used. To approximate $\cos(k_r \Delta x)$ the McClellan or Hazra and Reddy transformation can be used, but it is also possible to use the WLSQ optimization method described in section 8.3.1. Note that the coefficients in the Chebychev recursion scheme can also be optimized with the same method. The recursive convolution scheme of equation (8.37) is given in Figure 8.10. This scheme is

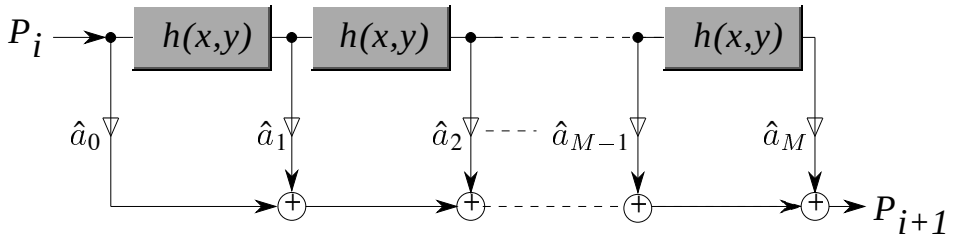

Fig. 8.10 *Direct scheme for series expansion in* $\cos(k_r \Delta x)$. *Note the simple structure in comparison with the Chebychev recursion scheme.*

less complicated to implement in the computer and more important it can be optimized better by the compiler (see section 8.6). In Figure 8.11a the impulse response is shown with the Hazra and Reddy optimized coefficients for the approximation to $\cos(k_r \Delta x)$. The number of terms is equal to 13. Note that with this method the results are better circular and contain only small artefacts even with the small (3x3 points) operator. In Figure 8.11b the series expansion in $\cos(k_r \Delta x)$ is done with an approximation to $\cos(k_r \Delta x)$ obtained with the WLSQ method introduced in section 8.3.1. Note that with a 9 point approximation to $\cos(k_r \Delta x)$ the result is accurate upto the higher angles. In the next subsection a detailed error analysis is given for all McClellan methods discussed.

8.4.4 Error analysis

Using the analysis technique, which was introduced by the direct method, it is possible to analyze the performance of the different McClellan transformations. In Table 8.3 the errors are given for five types of McClellan transformations; the original McClellan transformation in first and second order, the optimized Hazra & Reddy factors (HR) in first order, the non-linear optimized factors in the expanded second order and the series expansion in $\cos(k_r \Delta x)$ with the Hazra and Reddy coefficients and the WLSQ operators. From the results in the Table and Fig-

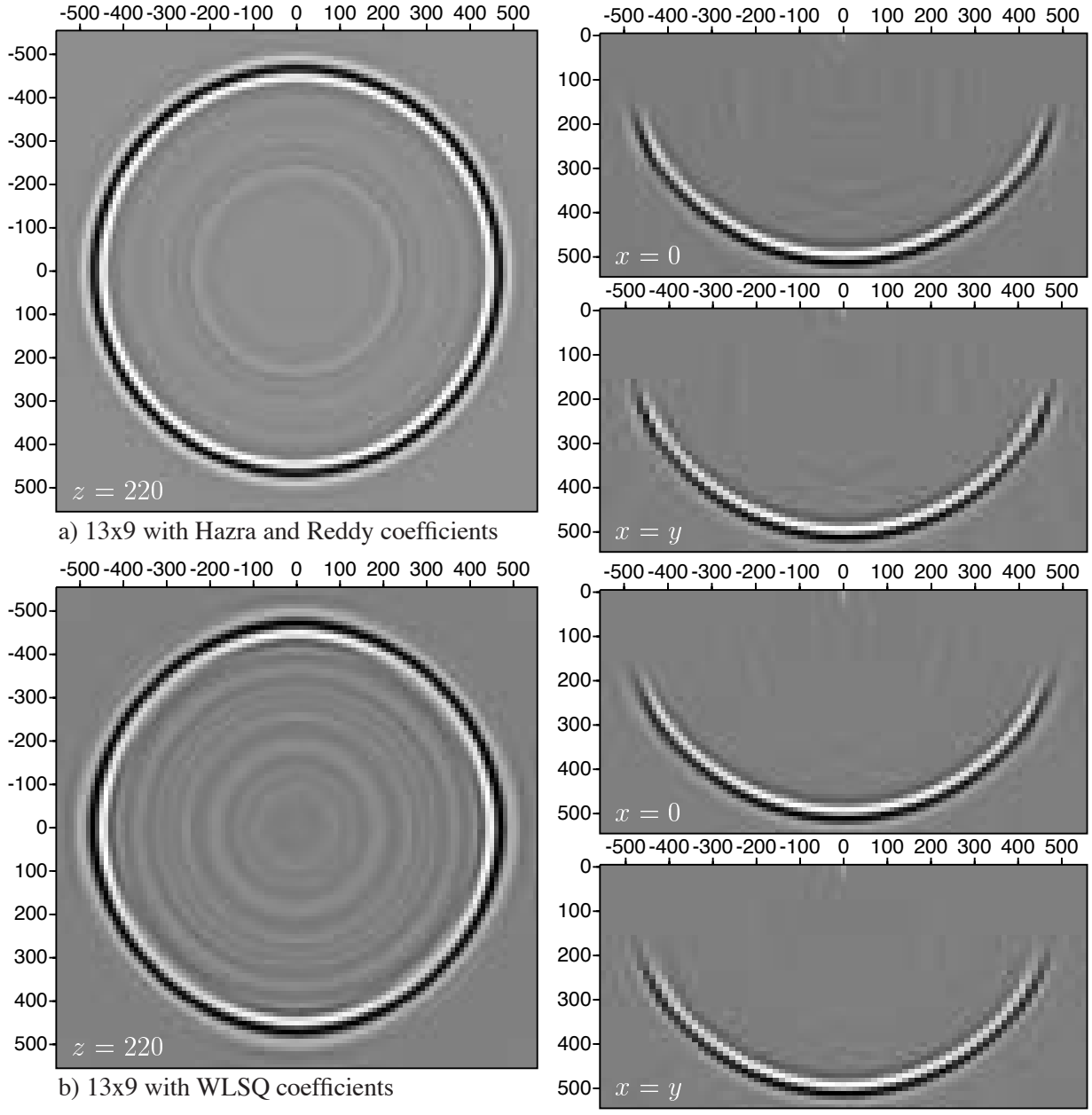

a) 13x9 with Hazra and Reddy coefficients

b) 13x9 with WLSQ coefficients

Fig. 8.11 *Impulse response of the expansion in* $\cos(k_r \Delta x)$ *Hazra and Reddy optimized coefficients for* $\cos(k_r \Delta x)$ *and WLSQ optimized coefficients. The series coefficients* $\hat{a}_m$ *in both examples are optimized by using the WLSQ method.*

ures 8.6, 8.8, 8.9, 8.11 the following remarks can be made;
(1) For higher frequencies the ε^p error in the original McClellan transformation increases significantly for both the first and second order approximation.
(2) The differences in pulse responses between the methods with, the original McClellan factors, the Hazra & Reddy factors, the non-linear optimized factors or the series expansion can be determined from the ε^p error. The second order method with the original McClellan factors give a rapidly increasing phase error where the largest errors occurs at the diagonal from $(0, 0)$ to $(k_{x,N}, k_{y,N})$. The phase error of the Hazra & Reddy method is less rapidly increasing and the

Operator	**5 Hz**			**20 Hz**			**40 Hz**		
McClellan	ε_2	ε^a_∞	ε^p	ε_2	ε^a_∞	ε^p	ε_2	ε^a_∞	ε^p
10x9	1.7e-3	1.0e-3	4.5e-4	6.6e-3	2.2e-3	4.8e-3	5.1e-2	1.5e-3	3.8e-2
13x9	1.4e-3	1.2e-3	3.2e-4	6.3e-3	1.7e-3	3.9e-3	5.2e-2	1.4e-3	3.8e-2
16x9	1.1e-3	1.3e-3	2.3e-4	6.3e-3	1.1e-3	3.7e-3	5.1e-2	1.6e-3	3.9e-2
10x17	1.7e-3	1.0e-3	4.4e-4	1.8e-3	2.4e-3	2.7e-3	2.4e-2	1.5e-3	2.2e-2
13x17	1.3e-3	1.2e-3	3.1e-4	1.1e-3	2.0e-3	1.4e-3	2.4e-2	1.6e-3	2.3e-2
16x17	1.1e-3	1.3e-3	2.3e-4	7.8e-4	1.4e-3	9.7e-4	2.4e-2	1.9e-3	2.3e-2
HR	**5 Hz**			**20 Hz**			**40 Hz**		
10x9	2.6e-3	1.2e-3	8.1e-4	7.2e-3	1.7e-3	2.8e-3	8.2e-2	7.7e-3	1.8e-2
13x9	1.2e-3	6.7e-4	2.9e-4	7.1e-3	2.7e-3	2.3e-3	8.2e-2	1.6e-2	1.8e-2
16x9	1.4e-3	1.4e-3	3.2e-4	7.2e-3	1.7e-3	1.9e-3	8.2e-2	2.7e-2	1.8e-2
Optimized	**5 Hz**			**20 Hz**			**40 Hz**		
10x25	1.7e-3	1.0e-3	4.4e-4	1.8e-3	2.4e-3	2.6e-3	7.2e-3	1.5e-3	9.4e-3
13x25	1.4e-3	1.2e-3	3.2e-4	1.2e-3	2.0e-3	1.4e-3	7.2e-3	1.9e-3	8.6e-3
16x25	1.1e-3	1.3e-3	2.3e-4	9.2e-4	1.4e-3	1.0e-3	7.2e-3	2.3e-3	8.5e-3
Series HR	**5 Hz**			**20 Hz**			**40 Hz**		
10x9	5.2e-3	2.5e-3	1.6e-3	1.7e-3	1.8e-3	2.5e-3	8.4e-3	2.3e-3	6.7e-3
13x9	2.0e-3	1.5e-3	5.3e-4	9.8e-4	1.3e-3	1.4e-3	8.4e-3	2.4e-3	5.6e-3
16x9	1.5e-3	7.7e-4	3.6e-4	6.4e-4	1.2e-3	8.4e-4	8.4e-3	2.2e-3	5.2e-3
Series WLSQ	**5 Hz**			**20 Hz**			**40 Hz**		
10x9	2.8e-3	1.8e-3	8.2e-4	5.1e-3	1.7e-3	3.8e-3	2.2e-3	2.3e-3	4.5e-3
13x9	1.3e-3	6.2e-4	3.4e-4	5.0e-3	1.4e-3	3.4e-3	2.0e-3	1.6e-3	3.6e-3
16x9	5.3e-4	3.4e-4	1.1e-4	5.0e-4	4.1e-4	3.2e-3	1.9e-3	4.2e-4	3.4e-3
10x25	2.2e-3	1.2e-3	6.4e-4	8.3e-4	8.4e-4	1.2e-3	1.4e-3	1.6e-3	2.8e-3
13x25	1.3e-3	4.1e-4	3.2e-4	4.3e-4	6.9e-4	5.9e-4	1.2e-3	1.2e-3	1.5e-3
16x25	5.7e-4	2.7e-4	1.2e-4	1.9e-4	2.9e-4	2.6e-4	1.1e-3	3.4e-3	1.4e-3

Table 8.3 *Errors in the extrapolation operators for; the original McClellan transformation in first (*x9) and second (*x17) order, the optimized Hazra & Reddy factors (HR) in first order, non-linear optimized factors in the expanded second order and the series expansion in* $\cos(k_r)$ *with the Hazra and Reddy coefficients and WLSQ operators. The maximum angle of interest is* 60^o.

smallest error is positioned at the diagonal from $(0,0)$ to $(k_{x,N}, k_{y,N})$. The non-linear optimized method gives error peaks at the edges of the domain of interest and has the largest error at the diagonal from $(0,0)$ to $(k_{x,N}, k_{y,N})$. The series expansion method with a WLSQ approximation to $\cos(k_r \Delta x)$ gives the smallest errors with error peaks at the edges on the k_x and k_y axes.

In Table 8.4 the shortest accurate operator is given as function of the maximum angle of interest. For small angles the original first order McClellan transformation in Chebyshev series gives already good results. For intermediate angles the second order McClellan scheme or the first order

Operator			40 Hz			Average		
angle	size	method	ε_2	ε^a_∞	ε^p	$\bar{\varepsilon}_2$	$\bar{\varepsilon}^a_\infty$	$\bar{\varepsilon}^p$
15	4x9	McC	1.7e-3	2.9e-3	1.5e-4	1.8e-3	2.0e-3	1.0e-4
30	5x9	McC	3.9e-3	2.0e-3	1.0e-3	3.1e-3	2.0e-3	5.4e-4
45	7x17	McC	5.2e-3	2.5e-3	3.3e-3	3.1e-3	2.0e-3	1.5e-3
60	10x9	Series	2.2e-3	2.3e-3	4.5e-3	3.4e-3	1.9e-3	3.0e-3
75	18x25	Series	6.9e-3	2.6e-3	2.6e-2	4.7e-3	1.9e-3	1.2e-2

Table 8.4 *Optimum operators which are accurate up to a maximum angle of interest.*

Hazra & Reddy factors are sufficient, for higher angles the series expansion with WLSQ optimized series coefficients gives the best results. The Hazra & Reddy factors have a large ε_2 for the higher frequencies due to stretching of the operator. For the 75^o angle a 5x5 approximation to $\cos(k_r \Delta x)$ is needed.

8.5 Double series expansion

By using a double series expansion in k_z, i.e. k_z is expanded in terms of $k_x^2 + k_y^2 (= k_r^2)$ (see equation (8.39)) ,

$$k_z = k\sqrt{1 - k_r^2} \approx k\,(1 - \frac{k_r^2}{2} - \frac{(k_r^2)^2}{8} - \frac{(k_r^2)^3}{16} - \frac{5\,(k_r^2)^4}{128} - \frac{7\,(k_r^2)^5}{256} + \mathrm{O}((k_r^2)^6) \tag{8.39}$$

there is an extra advantage (Berkhout, 1982). The basic spatial convolution operators are reduced to the simple 1-D convolution operators: $d_2(x)$ and $d_2(y)$. The terms of the series expansion can be derived from the Taylor series but this is not an optimum choice (Hoff, 1995). The same expansion can also be regarded as an approximation to the cosine terms in equation (8.23). So there are two different ways to look at the double series expansion

$$\tilde{F}_0(k_x, k_y) = \exp(-jk_z \Delta z) \tag{8.40}$$

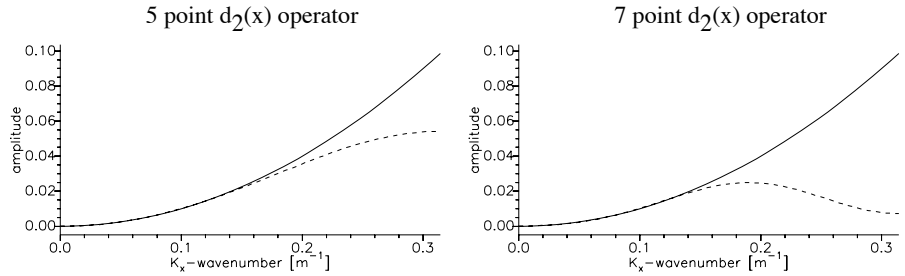

Fig. 8.12 *Spectrum of two differentiation operator for 5 and 7 points. The maximum wavenumber of interest is given by* $k_{max} = \frac{2\pi 25}{1000} \approx 0.16$.

$$\approx \sum_{m=0}^{M} a_m T_m(\cos(k_r)) \tag{8.41}$$

$$\approx \sum_{m=0}^{M} b_m T_m(k_r) \tag{8.42}$$

$$\approx \sum_{m=0}^{M} c_m k_r^m \tag{8.43}$$

where T_m is a Chebyshev polynomial of the m'th order. In subsection 8.5.1 equation (8.43) is regarded with the series expansion scheme. In subsection 8.5.2 equation (8.42) is discussed with the Chebyshev recursion scheme.

8.5.1 Expansion in $k_x^2 + k_y^2$ with L_2-norm

The short spatial operator of k_x^2 and k_y^2, i.e. $d_2(x)$ and $d_2(y)$, are determined by a weighted least-squares process. In Figure 8.12 two wavenumber spectra are shown for spatial convolution operators, with operator lengths of 5 and 7 points, which represent the second order differentiation. Note that for these short operators the approximation to the exact function within the band of interest is within a reasonable error. The convolution scheme of this expansion is given in Figure 8.13 where $d_2(x, y)$ stands for the spatial Laplacian operator $d_2(x)+d_2(y)$. The factors $\hat{b}_m$ of the series expansion in Figure 8.13 are obtained by a weighted least-squares optimization method with respect to the wavenumber spectrum of the *optimized* $k_x^2 + k_y^2$ operator. The length of the 1-D convolution operators depends on the maximum wavenumber of interest (Hoff, 1995).

Hoff (1995) showed that the value of the coefficients in the series expansion grows rapidly with increasing order. For the higher order terms values in the order of 1e19 are normal. This means that after a certain number of terms the accuracy cannnot be improved any further.

The scheme proposed in this section is similar to that of Sollid and Arntsen (1994), but there are some small differences; to obtain the series coefficients the whole wavenumber spectrum is used while Sollid and Arntsen use only the diagonal $(0, 0)$ to $(k_{x,N}, k_{y,N})$. For the least squares optimization we use a (fast) WLSQ scheme while Sollid and Arntsen use a non-linear scheme and finally the implementation is done in a series expansion and not in an Chebychev recursion scheme.

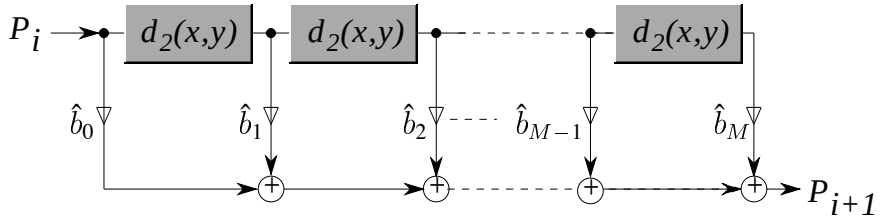

Fig. 8.13 *Series expansion in terms of $k_x^2 + k_y^2 = \tilde{L}$. The $d_2(x, y)$ boxes represent the two 1-D convolutions with the optimized Laplacian operator, the $\hat{b}_m$ represent the optimized coefficients in the series expansion.*

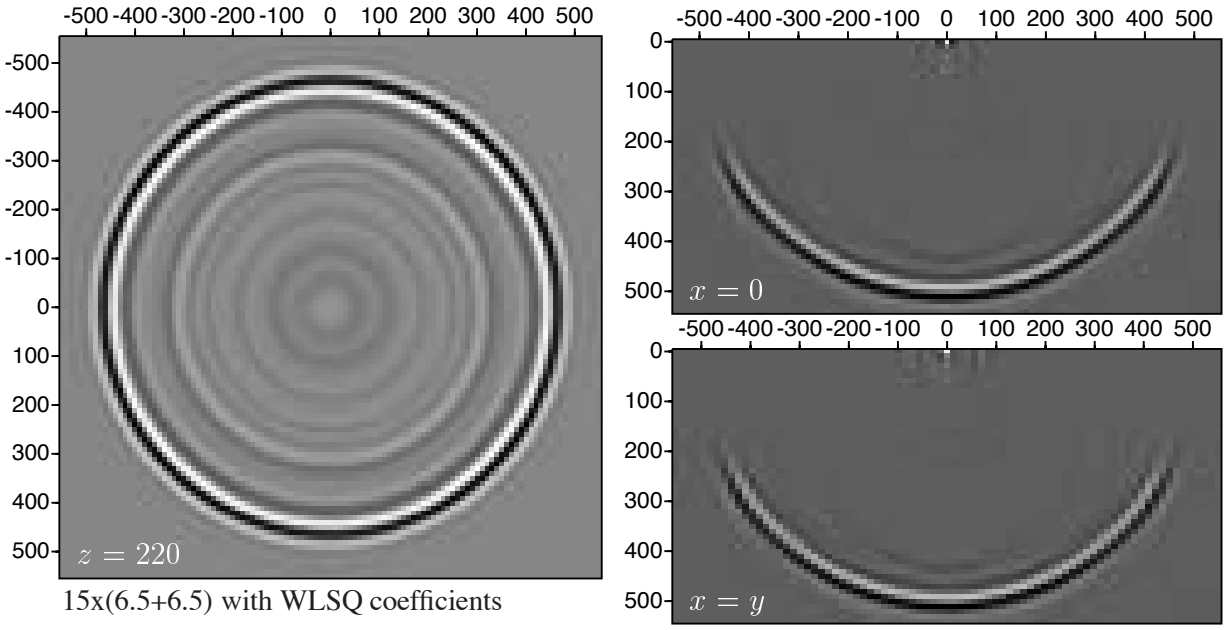

Fig. 8.14 *Depth images of pulse responses obtained with the series expansion in $k_x^2 + k_y^2$.with a basis operator with optimized operator lengths with 15 terms in the series expansion (example provided by Jochum Hoff).*

In Figure 8.14 the impulse responses is shown for a 3,5,7,9,11 combination with 15 coefficients. The impulse response shows artefacts at the higher angles which are due to edge effects of the used WLSQ method. In WLSQ design the edges of the domain of interest contain relative large error peaks. It may therefore be better to use an L_∞ norm in the design of the series coefficients. In the next subsection this second approach, after Soubaras, with a Chebychev recursion scheme is explained.

8.5.2 Expansion in $k_x^2 + k_y^2$ with L_∞-norm

Soubaras (1992) used the same type of expansion in $k_x^2 + k_y^2$, but in his method the optimization technique for both the terms in the series expansion and the convolution operators is the Remez exchange algorithm with the L_∞ norm. The advantage of the Chebyshev recursion scheme, given in Figure 8.15 over the series expansion, which was discussed in the previous subsection, is that the coefficients in the Chebyshev expansion are less sensitive to numerical errors. A disadvantage of the Chebyshev scheme are the increasing number of additions needed.

Optimization of the differentiation operators with the L_∞ norm gives equiripple operators. Optimization of the series expansion terms with the L_∞ norm can be done by reducing the polynomial synthesis to symmetrical spectral synthesis with the aid of a simple transformation (McClellan and Chan, 1977). In this transformation only the extreme values of the wavenumber spectrum of the differentiation operator are used in the optimization and not, as with the L_2 optimization the whole spectrum of the differentiation operator. The transformation from polynomials to spectral synthesis reduces the 2-D optimization problem to a 1-D optimization problem which can be solved with the Remez exchange algorithm in a fast way. In the extrapolation

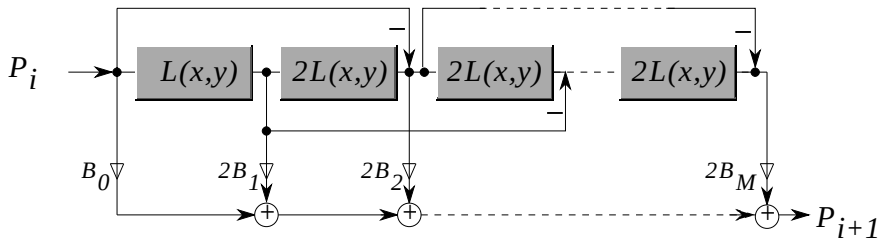

Fig. 8.15 *Expansion in terms of $k_x^2 + k_y^2 = \tilde{L}$. The $d_2(x, y)$ boxes represent the two 1-D convolutions with the optimized L operator, the B_m represent the optimized coefficients in the series expansion.*

scheme the differentiation operator remains the same for all frequencies. However, the terms in the series expansion are calculated for every frequency.
In Figure 8.16 one impulse response is shown for a 7+7 point operator with 15 terms in the expansion. The impulse response has a circular response with only small artefacts at the lower wavenumbers.

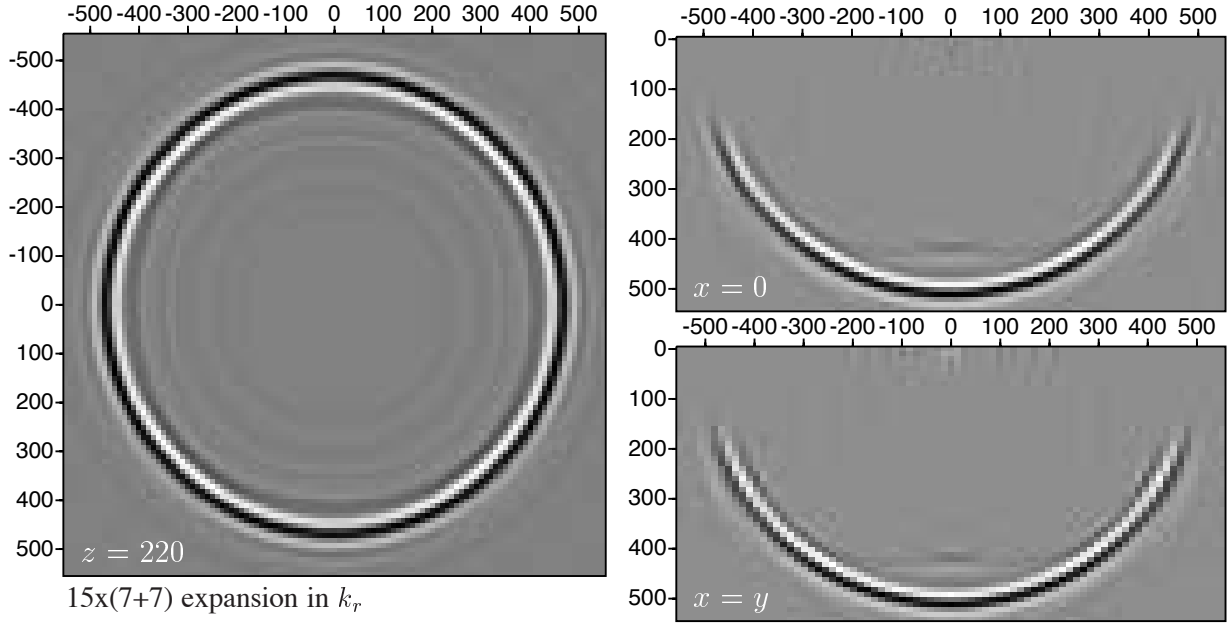

Fig. 8.16 *Depth images of impulse response obtained with the series expansion in $k_x^2 + k_y^2$ with L_∞ optimization; a 7 point 1D convolution operator with 15 terms in the Chebyshev expansion.*

8.5.3 Error analysis

In Table 8.5 the errors are given for the series expansion in $k_x^2 + k_y^2$ implemented in a direct recursion scheme with L_2 optimization and the Chebyshev recursion scheme with L_∞ optimization. From the results in the Table the following remarks can be made;
(1) In both optimization methods the number of terms is less essential to the accuracy than the

size	**5 Hz**			**20 Hz**			**40 Hz**		
Direct	ε_2	ε^a_∞	ε^p	ε_2	ε^a_∞	ε^p	ε_2	ε^a_∞	ε^p
10x(3,5,7)	5.8e-3	1.9e-3	1.8e-3	3.2e-3	3.7e-3	4.6e-3	3.4e-3	3.4e-3	6.4e-3
12x(3,5,7)	6.1e-3	2.8e-3	1.9e-3	3.0e-3	3.2e-3	4.1e-3	3.1e-3	3.4e-3	5.1e-3
15x(3,5,7)	6.1e-3	3.5e-3	1.9e-3	2.4e-3	3.2e-3	3.3e-3	3.0e-3	3.9e-3	4.8e-3
Chebyshev	**5 Hz**			**20 Hz**			**40 Hz**		
10x(7+7)	4.0e-2	3.7e-3	2.3e-3	7.1e-3	3.0e-3	4.5e-3	4.3e-3	1.9e-3	6.5e-3
12x(7+7)	4.0e-2	7.6e-3	2.1e-3	7.1e-3	5.0e-3	4.4e-3	4.1e-3	4.9e-3	5.8e-3
15x(7+7)	4.0e-2	1.2e-2	2.4e-3	6.8e-3	5.8e-3	3.4e-3	4.1e-3	6.5e-3	5.0e-3

Table 8.5 *Errors in the extrapolation operators for the direct series expansion in $k_x^2 + k_y^2$ and a Chebyshev recursion scheme in $k_x^2 + k_y^2$. The maximum angle of interest is 60^o.*

length of the d_2 operator. Increasing the number of terms improves the result only a little, while increasing the length of the d_2 operator gives a significant improvement on the result.
(2) The artefacts present in the impulse response with the series expansion scheme are due to instabilities at the higher angles. This effect is due to the use of the L_2 norm optimization (Hoff, 1995). In the L_∞ norm optimization unstable error peaks are not likely to occur. The artefacts in the L_2 optimization can be removed with an additional optimization step.
(3) Although the ε_2 errors for the lower frequencies in the L_∞ norm optimization are larger than the errors in the L_2 norm optimization the impulse response contains less artefacts. However, the amplitude of the spatial impulse repsonse in the L_∞ norm optimization is less accurate.

In Table 8.6 the shortest accurate operator in L_∞ optimization is given as function of the maximum angle of interest. The ε_2 error is the most sensitive error in the L_∞ optimization. For 15^o and 30^o angle the same number of terms must be used, a lower number of terms leads to unacceptable ε_2 errors for the low and middle frequencies. The optimum operator size can be found by trying to make the ε_2 as small as possible by choosing the number of terms high. The optimum number of terms is then found by lowering the number of terms until the ε_2 is changing significant. The high average errors are due to the high errors at 5 Hz. For a maximum angle of 75^o it is not possible to obtain stable operators for reasonable operator sizes.

Operator		**20 Hz**			**Average**		
angle	size	ε_2	ε^a_∞	ε^p	$\bar{\varepsilon}_2$	$\bar{\varepsilon}^a_\infty$	$\bar{\varepsilon}^p$
15	5x(7+7)	8.6e-3	5.1e-3	1.7e-4	9.6e-3	9.7e-3	5.0e-4
30	5x(7+7)	3.0e-3	1.9e-3	3.9e-3	1.2e-2	6.1e-3	3.7e-3
45	7x(7+7)	5.0e-3	4.5e-3	2.0e-3	1.5e-2	5.8e-3	1.0e-2
60	9x(7+7)	8.3e-3	1.8e-3	6.3e-2	1.7e-2	2.3e-3	4.0e-2

Table 8.6 *Optimum operators which are accurate up to a maximum angle of interest.*

8.6 Computation times

The computation times of the different 3-D extrapolation methods in the space-frequency domain discussed in this chapter are given in table 8.7. The given time represent 55 recursive depth steps for one frequency (20 Hz.) with $c = 1000ms^{-1}, \Delta x = \Delta y = \Delta z = 10m$ on a x,y grid of 111×111 samples wide. All routines which are used are written in C and Fortran and are translated with the same type of compiler options without using options for parallel computation (see Table 8.8). However, parallel processing is easily implemented on the main frequency loop in the extrapolation algorithm. On the Convex (C-220) the -O2 option is used for vectorization of

	Direct			**McClellan 1**			**McClellan 2**		
Machine	19x19	25x25	31x31	10x9	13x9	16x9	10x17	13x17	16x17
SUN C	63.5	104.6	157.3	24.5	31.1	38.7	33.4	44.8	55.3
SUN F	52.6	88.0	144.8	20.3	27.0	31.7	28.8	39.0	47.8
Convex F	34.7	61.9	85.9	12.4	17.4	21.6	21.1	27.6	33.5
DEC C	28.3	46.9	71.6	9.4	13.7	15.7	13.4	17.8	21.5
DEC F	11.5	19.9	28.0	5.6	7.2	8.8	6.7	8.6	10.5
HP C	18.6	30.0	44.7	10.0	13.2	16.5	20.5	23.5	27.7
HP F	6.8	10.6	15.1	6.6	8.6	10.6	19.2	20.8	24.5
	McClellan 2+			$\cos(k_r \Delta x)$ $\times 9$			$\cos(k_r \Delta x)$ $\times 25$		
Machine	10x25	13x25	16x25	10x9	13x9	16x9	10x25	13x25	16x25
SUN C	41.9	55.0	67.2	18.0	23.5	29.2	35.0	45.9	59.9
SUN F	36.8	48.0	58.3	16.8	21.1	25.7	32.6	42.9	54.3
Convex F	33.4	45.5	54.1	11.6	16.2	18.5	34.0	42.3	53.9
DEC C	14.6	18.5	24.3	7.0	9.3	10.8	12.1	15.6	19.2
DEC F	7.5	9.6	11.8	4.4	5.6	6.7	6.2	7.9	9.6
HP C	23.3	26.4	30.4	7.9	10.3	12.3	13.4	17.0	20.8
HP F	15.1	18.2	22.0	4.0	5.1	6.2	12.2	14.6	17.4
	k_z			$k_x^2 + k_y^2$ L_2			$k_x^2 + k_y^2$ L_∞		
Machine	10x(5x5)	15x(5x5)	10x(7x7)	12x5	12x7	15x7	12x5	12x7	15x7
SUN C	36.3	54.3	61.2	25.7	32.8	41.2	33.4	41.9	51.7
SUN F	33.2	49.0	57.2	21.2	26.2	35.5	27.9	32.0	39.9
Convex F	31.5	49.6	71.1	15.1	19.7	24.3	19.0	24.2	30.0
DEC C	11.8	17.6	26.3	8.6	9.6	11.9	13.6	15.2	19.2
DEC F	6.2	9.1	8.5	5.6	5.6	6.8	7.0	7.7	9.8
HP C	12.8	18.8	18.5	15.9	21.4	27.4	14.6	18.1	22.3
HP F	9.5	14.7	20.1	13.5	20.0	25.3	11.8	15.8	18.3

Table 8.7 *2-D convolution computation time (in seconds) for one frequency on different machines for different operator sizes and extrapolation methods.*

the loops. It was not possible to vectorize the C-code with specific compiler directives, therefore the convolution schemes were written in Fortran code which vectorizes well. Note that the Fortran compilers are better in optimization than the C compilers.
In the direct implementation of the 2-D convolution the even symmetry in the convolution operator is used. This implementation is designed to work fast on a Vector computer. In the implementation of the McClellan transformation and the k_z expansion the circular symmetry in the basis operators is used by first adding the common terms to each other and then multiplication with the appropriate operator point. This reduces the number of multiplications with a factor 8 in comparison with a full convolution. The computation times given in Table 8.7 are real-time computation times measured during the calculation. The time needed to calculate the operators is not included in this time.

Due to the use of the even symmetry in the operator the computation time for the direct convolution is a real challenge for the other methods (Note that the direct scheme can be made even faster when $\Delta x = \Delta y$ and the circular symmetry is used). The first and second order McClellan implementations and the series expansion in $\cos(k_r \Delta x)$ are the fastest algorithms on all machines. The series expansion in k_z and in $k_x^2 + k_y^2$ are comparable with the McClellan transformation. The difference between the $k_x^2 + k_y^2$ expansion in L_2 and L_∞ is that in the L_2 scheme the direct series expansion is used and for the L_∞ the Chebyshev recursion scheme is used. From the table it is clear that the hardware design of the computer system can be optimum for some specific implementation. For example the HP has a good performance on the direct scheme and less on the McClellan schemes. The DEC has a good performance on all expansion schemes.
Which scheme is preferred depends also on the desired accuracy of the result. If one uses the extrapolation only to get a first idea of the subsurface, or to estimate the macro model, a first order McClellan can be used. For a higher accuracy the direct convolution or a series expansion method with a high number of terms can be used.

Machine	type	RAM	bits	C	F	C-opt	F-opt
SUN	10/514	256	32	gcc	f77	-O2	-O2
Convex	C-220	256	32	cc	fc	-O2	-O2
DEC	3000-500	96	64	cc	f77	-O2	-O3
HP	9000-735	144	32	cc	fort77	+O4	+O4

Table 8.8 *Specification for the used machines. Note that the optimization is done for one CPU and parallel processing is not used.*

In Table 8.8 a detailed specification for the different machines is given. On the SUN the gcc compiler is used because it produces faster code than the standard cc compiler delivered by SUN. Note that for the optimization options only the most common used options are chosen, it may therefore be possible that by choosing another option the scheme will perform better as described in this section (suggestions for better options are welcome).

8.7 Discussion and Conclusions

The 3-D extrapolation algorithm that is used in recursive depth migration can be implemented in several ways. In this Chapter the direct method, the McClellan transformation and two series expansion methods have been discussed. For the direct method a 2-Dimensional convolution operator is needed. The proposed weighted least-squares optimization method is an efficient procedure which gives stable and accurate convolution operators (Thorbecke and Rietveld, 1994). This method can be further improved by a second optimization step; for example, the Lawson algorithm (Rice and Usow, 1968), which will adjust the weight function in such a way that after several steps it will converge to a Chebyshev-norm solution; see for example Algazi et al. (1986).

The McClellan scheme, which makes use of the 1-D optimized operator coefficients, is attractive with respect to the computation effort and by using optimized McClellan factors the accuracy for the higher angles can be improved significantly without much effort. Using a series expansion of the phase shift operator also reduces the computation time in comparison with a direct 2-Dimensional convolution. These different approaches to the phase shift operator can be summarized in the following equations

$$\tilde{F}_0(k_x,k_y) = \exp\left(-jk_z\Delta z\right) \tag{8.44}$$

$$\approx \sum_{m=0}^{M}\sum_{n=0}^{N} F_{mn}\cos\left(k_x m\Delta x\right)\cos\left(k_y n\Delta y\right) \tag{8.45}$$

$$\tilde{F}_0(k_x,k_y) \approx \sum_{m=0}^{M} F_m T_m(\cos\left(\sqrt{k_x^2+k_y^2}\Delta x\right)) \tag{8.46}$$

$$\approx \sum_{m=0}^{M} a_m \cos^m\left(\sqrt{k_x^2+k_y^2}\Delta x\right) \tag{8.47}$$

$$\tilde{F}_0(k_x,k_y) \approx \sum_{m=0}^{M} B_m T_m(k_x^2+k_y^2) \tag{8.48}$$

$$\approx \sum_{m=0}^{M} b_m (k_x^2+k_y^2)^m \tag{8.49}$$

$$\tilde{F}_0(k_x,k_y) \approx \sum_{m=0}^{M} C_m T_m(k_z) \tag{8.50}$$

$$\approx \sum_{m=0}^{M} c_m k_z^m \tag{8.51}$$

with

$$\cos\left(\sqrt{k_x^2+k_y^2}\right) \approx \sum_{p=0}^{P}\sum_{q=0}^{Q} c_{pq}\cos\left(pk_x\right)\cos\left(qk_y\right) \tag{8.52}$$

$$\cos\left(\sqrt{k_x^2+k_y^2}\right) \approx a_0 + b_1\sqrt{k_x^2+k_y^2}. \tag{8.53}$$

Equation (8.45) represents the direct method, equation (8.46) combined with equation (8.52) is the McClellan approach with the Chebyshev recursion scheme. Equation (8.47) is the series

expansion in $\cos(k_r \Delta x)$ with a dependent optimization between the series coefficients and the approximation to $\cos(k_r \Delta x)$. Equation (8.48) with equation (8.53) is the expansion in $k_x^2 + k_y^2$ with the Chebyshev recursion scheme. Equation (8.49) is the series expansion in $k_x^2 + k_y^2$; the use of this series expansion in recursive migration was already proposed by Berkhout (1982). Equation (8.50) represents the expansion in k_z in a Chebychev recursion scheme and Equation (8.50) the series expansion in k_z.

From an efficiency point of view the expansion in $k_x^2 + k_y^2$ (8.49) and the use of the McClellan transformation (8.46) are the two most interesting schemes. An extra advantage of the expansion in $k_x^2 + k_y^2$ is that short 1-Dimensional convolution operators can be used. A disadvantage of these schemes is that it is not possible to write the algorithms in a computer 'friendly' way due to the recursive structure in the scheme. This fact is displayed in the computation times given in section 8.6. The most accurate extrapolation is the direct convolution scheme. Another advantage of the direct scheme is that the algorithm can be designed in an efficient way. A disadvantage of the direct scheme is the intensive computation of the 2-D convolution operators.

The approximation to $\cos(k_r \Delta x)$ can be done with many different methods. Crucial in the performance of the extrapolation operator is that the coefficients in the expansion (Chebyshev or series) are optimized by using the approximation to $\cos(k_r \Delta x)$.

Method	**accuracy**	**stable**	**circ**	**operator**	**simple**	**vector**	**scalar**
Direct	++	+	++	-	++	+	+
McC1	o	++	o	+	o	+	++
McC2	o	++	o	+	o	+	++
McC2+	+	+	+	+	-	+	+
$\cos(k_r \Delta x)$	+/++	+	++	o	+	+	++
k_z	-	o	o	o	+	-	o
$k_x^2 + k_y^2$ L_2	o	o	+	+	o	o	+
$k_x^2 + k_y^2$ L_∞	o	+	+	++	-	o	+

Table 8.9 *Comparison of the different extrapolation methods with respect to computation effort and stability. Note that in the McClellan schemes the optimized McClellan factors are used.*

A more detailed overview of the pros and cons of the different methods is given in Table 8.9. In this table the different columns have the following meaning:

• *accuracy*: the average ε_2 error over the whole frequency range.

• *stable*: the stability of the method over the whole frequency range for all wavenumbers (ε_∞^a error). A o means that some wavenumber components can become unstable.

• *circ*: the circularity of the impulse response (ε^p error). The McClellan in Chebychev expansion and the k_z scheme have problems with the circulariry.

• *operator*: the effort to compute all the coefficients which are needed in the convolution scheme. For example in the direct method a 2-D convolution operator must computed, in the McClellan

scheme a 1-D convolution operator and the (optimized) McClellan factors are needed. In the table ++ means a minimum computation effort to compute the coefficients. Note that the operator coefficients can be calculated in advance and stored in an operator table.
• *simple*: the simplicity of the implementation of the convolution. The recursive schemes require more complex algorithms, so the compilers have to be good in optimization to make these schemes fast. In the recursive schemes it is difficult to make the program faster by changing the algorithm in a more computer 'friendly' way. A direct convolution requires more multiplications and additions but the algorithm can be made very efficient. This fact explains the fast computation time of the direct scheme in comparison with the other schemes (see section 8.6).
• *vector*: the performance of the scheme on a vector computer. The direct scheme is the only scheme which can be implemented in a vector efficient way.
• *scalar*: the performance of the scheme on a modern scalar computer. Note that some scalar computers may have an architecture which can be more advantageous for some implementations.

In conclusion taking into account the *computation time* of the different methods, the *simplicity* of the algorithms and most important the *accuracy* of the result then the **direct method** (8.45) is the best method for 3D extrapolation. The 2-D convolution operators should be stored in an efficient way, by using the even symmetry of the operator (one octant need be stored only), in an operator table that can be calculated in advance. Note that our algorithm of the direct scheme can be made faster by also taking the circular symmetry (if $\Delta x = \Delta y$) of the operator into account.

If a series expansion version is used we prefer the expansion in $\cos(k_r \Delta x)$ (8.47). It is our opinion that Chebychev recursion is not an advantage.

8.8 References

Algazi, V. R., Suk, M., and Rim, C. S., 1986, Design of almost minimax fir filters in one and two dimensions by wls techniques: IEEE Trans. Circuits and Systems, **CAS-33**, 590–596.

Berkhout, A. J., 1982, Imaging of acoustic energy by wave field extrapolation (2nd edition): Elsevier Amsterdam.

Berkhout, A. J., 1984, Seismic resolution; resolving power of acoustical echo techniques (volume 12): Geophysical Press.

Biondi, B., and Palacharla, G., 1994, 3d depth migration using rotated mcclellan filters: 56th Mtg. Vienna, EAEG, Expanded Abstracts of Papers, B45.

Blacquière, G., Debeye, H. W. J., Wapenaar, C. P. A., and Berkhout, A. J., 1989, 3d table-driven migration: Geophysical Prospecting, **37**, 925–958.

Blacquière, G., 1989, 3d wave field extrapolation in seismic depth migration: Ph.D. thesis, Delft University of Technology.

Blacquière, G., 1991, Optimized mcclellan transformation filters applied in one-pass 3-d depth migration.: 61th Ann. Internat. Mtg., SEG, Expanded Abstracts, 1126–1129.

Gaiser, J. E., 1994, Optimum transformation and filter structure for explicit finite-difference 3d migration: 56th Mtg. Vienna, EAEG, Expanded Abstracts of Papers, B42.

Gazdag, J., 1978, Wave equation migration with the phase-shift method: Geophysics, **43**, 1342–1351.

Hale, D., 1991a, 3-d depth migration via mcclellan transformations: Geophysics, **56**, 1778–1785.

——– 1991b, Stable explicit extrapolation of seismic wavefields: Geophysics, **56**, 1770–1777.

Hazra, S. N., and Reddy, M. S., 1986, Design of circularly symmetric low-pass two-dimensional fir digital filters using transformation: IEEE Trans. Circuits and Systems, **CAS-33**, 1022–1026.

Hoff, J. D., 1995, 3d one-way wave field extrapolation by using 1d convolution operators: M.Sc. thesis, Delft University of Technology.

Holberg, O., 1988, Towards optimum one-way wave propagation: Geophysical Prospecting, **36**, 99–114.

Johnson, L. W., and Riess, R. D., 1977, Numerical analysis: Addison-Wesley.

Kao, J., G.Li, and C.Yang, 1994, Optimized 2d filters for 3d wavefield extrapolation on the massively parallel processors: 56th Mtg. Vienna, EAEG, Expanded Abstracts of Papers, B48.

Kogbetliantz, E. G., 1960, Generation of elementary functions:, *in* Mathematical Methods for Digital Computers New York: John Wiley & Sons, Selected Reprint, 1, 7–35.

McClellan, J. H., and Chan, D. S. K., 1977, A 2-d fir filter structure derived from the chebychev recursion: IEEE Trans. Circuits and Systems, **CAS-24**, 372–378.

McClellan, J. H., 1973, The design of two-dimensional digital filters by transformations: 7th Ann.Mtg, Princeton, Princeton Conf. on Inform. Sci. and Sys., 247–251.

Mersereau, R. M., Mecklenbräuker, W. F. G., and Quatieri, T. F., 1976, Mcclellan transformations for two-dimensional digital filtering: I-design: IEEE Trans. Circuits and Systems, **CAS-23**, 405–413.

Nautiyal, A., Gray, S. H., Whitmore, N. D., and Garing, J. D., 1993, Stability versus accuracy for an explicit wavefield extrapolation operator: Geophysics, **58**, 277–283.

Parks, T. W., and Burrus, C. S., 1987, Digital filter design: New York: John Wiley & Sons.

Powell, M. J. D., 1981, Approximations theory and methods: Cambridge University Press.

Ralston, A., 1967, Rational chebyshev approximation:, *in* Mathematical Methods for Digital Computers New York: John Wiley & Sons, Selected Reprint, 2, 264–285.

Rice, J. R., and Usow, K. H., 1968, The lawson algorithm and extensions: Math. Comp., **22**, 118–127.

Sollid, A., and Arntsen, B., 1994, Cost-effective 3d one-pass depth migration: Geophysical Prospecting, **42**, 755–776.

Soubaras, R., 1992, Explicit 3-d migration using equiripple polynomial expansion and laplacian synthesis: 62th Ann. Internat. Mtg., SEG, Expanded Abstracts, 905–908.

Thorbecke, J. W., and Rietveld, W., 1994, Optimum extrapolation operators: a comparison: 56th Ann. Internat. Mtg., EAEG, Expanded Abstracts, P105.

Thorbecke, J. W., 3d wave field extrapolation; a comparison between different methods:, Available from internet at http://wwwak.tn.tudelft.nl/ jan/articles/3Doperators.ps.Z, januari 1995.

Contents